

PACIFIC EARTHQUAKE ENGINEERING RESEARCH CENTER

Aftershock Seismic Vulnerability and Time-Dependent Risk Assessment of Bridges

Sujith Mangalathu

Mehrdad Shokrabadi

Henry V. Burton

Department of Civil and Environmental Engineering
University of California, Los Angeles

PEER Report No. 2019/04
Pacific Earthquake Engineering Research Center
Headquarters at the University of California, Berkeley

May 2019

Disclaimer

The opinions, findings, and conclusions or recommendations expressed in this publication are those of the author(s) and do not necessarily reflect the views of the study sponsor(s), the Pacific Earthquake Engineering Research Center, or the Regents of the University of California.

Aftershock Seismic Vulnerability and Time-Dependent Risk Assessment of Bridges

**Sujith Mangalathu
Mehrdad Shokrabadi
Henry V. Burton**

Department of Civil and Environmental Engineering
University of California, Los Angeles

PEER Report No. 2019/04
Pacific Earthquake Engineering Research Center
Headquarters at the University of California, Berkeley
May 2019

ABSTRACT

The time-dependent seismic risk of bridges is assessed while accounting for the effect of aftershocks and the uncertainty in the damage state after a mainshock event. To achieve this, a Markov risk-assessment framework is adopted to account for the probabilistic transition of the bridge structure through different damage states and time-dependent aftershock hazard. The methodology is applied to three typical California bridge configurations that differ only based on their era of design and construction. Era 11, Era 22, and Era 33 designations are used for the three bridges, which are designed and detailed to reflect pre-1971, 1971–1990 and post-1990 construction. In addition to mainshock-only evaluations (used as a benchmark to quantify the additional risk posed by aftershocks), pre-mainshock (to account for the uncertainty in the occurrence of mainshock and aftershock events) and post-mainshock (which are based on a conditioning mainshock event and bridge damage state) seismic risk assessments are performed. To support these assessments, a set of 34 pairs of ground motions from as-recorded mainshock–aftershock sequences is assembled. Sequential nonlinear response history analyses (including incremental dynamic analyses) are used to obtain the response demands when the structural models of all bridges are subjected to mainshock-only records or mainshock–aftershock record-pairs. Physical damage in both the mainshock and mainshock–aftershock environments is defined using the following mutually exclusive and collectively exhaustive limit states: Intact, Slight, Moderate, Extensive, and Complete. For both the pre- and post-mainshock assessments, the additional risk caused by aftershock hazard is found to be higher for the older bridges (i.e., Era 11 and Era 22) and more severe conditioning damage states. A direct correlation between the bridge’s age and the increase in seismic risk due to aftershock hazard was also observed for the pre-mainshock assessment. It is suggested that the proposed methodology be used to make informed decisions regarding the appropriateness and timing of bridge closures (partial and complete) following a seismic event while considering aftershock hazard.

ACKNOWLEDGMENTS

This work was funded under the PEER TSRP Fund No. 1137-NCTRHB from the State of California's Transportation Division-State Highway Fund, via the University of California Office of the President. Any opinions, findings, and conclusions or recommendations expressed in this material are those of the authors and do not necessarily reflect those of the sponsors, the Pacific Earthquake Engineering Research Center (PEER), or the Regents of the University of California.

CONTENTS

ABSTRACT	iii
ACKNOWLEDGMENTS	v
TABLE OF CONTENTS	vii
LIST OF TABLES	ix
LIST OF FIGURES	xi
1 INTRODUCTION.....	1
2 GROUND-MOTION SELECTION AND PROBABILISTIC SEISMIC HAZARD ANALYSIS	5
2.1 Introduction.....	5
2.2 Record Pairs for Response History Analysis.....	7
2.3 Probabilistic Seismic Hazard Analysis.....	10
3 MARKOV-BASED RISK ASSESSMENT FRAMEWORK	13
4 BRIDGE NONLINEAR STRUCTURAL MODELING AND LIMIT STATE DEFINITIONS	17
4.1 Introduction.....	17
4.2 Numerical Modeling	17
4.2.1 Substructure	17
4.3 Case Study Bridge Configurations	21
4.4 Limit States: Definitions.....	22
5 DEMONSTRATION OF THE PROPOSED FRAMEWORK.....	25
5.1 Mainshock and Aftershock Fragility Curves	25
5.2 Assessing Bridge Aftershock Seismic Risk in the Pre- and Post- Mainshock Environments	27
6 SUMMARY AND CONCLUSIONS	33
REFERENCES.....	35

LIST OF TABLES

Table 2.1	Attributes of the mainshock-aftershock ground-motion sequences.....	8
Table 4.1	Limit state descriptions for bridge columns [Mangalathu 2017].....	23
Table 5.1	Median (μ) and Dispersion (β) for mainshock and aftershock limit state fragility functions.....	26
Table 5.2	Conditional limit-state occurrence probabilities for the Era 11 bridge, 30 days after the mainshock.....	28
Table 5.3	Conditional limit-state occurrence probabilities for the Era 22 bridge, 30 days after the mainshock.....	29
Table 5.4	Conditional limit-state occurrence probabilities for the Era 33 bridge, 30 days after the mainshock.....	29
Table 5.5	Mean annual frequency of limit-state exceedance in the pre-mainshock environment.	31
Table 5.6	Limit state occurrence probabilities at the end of the assumed 50-year service life.	31

LIST OF FIGURES

Figure 2.1	Comparing the spectra of mainshock and aftershock records with similar magnitudes obtained from the Chiou and Youngs [2008] GMM.	7
Figure 2.2	Individual and median response spectra for the mainshock ground motions.....	9
Figure 2.3	Individual and median response spectra of aftershock ground motions.	9
Figure 2.4	Mainshock and aftershock (for 1 year after the occurrence of the mainshock) seismic hazard curves for $T = 1.0$ sec.....	11
Figure 4.1	Numerical modeling of various bridge components.....	18
Figure 4.2	Finite-element discretization of a single-column bent.	19
Figure 4.3	Shear key model.....	20
Figure 4.4	Analytical model of pounding between the deck and abutment back wall.....	21
Figure 4.5	Schematic illustration of the bridge layout.	22
Figure 5.1	Comparing mainshock and aftershock fragility curves corresponding to the (a) Slight, (b) Moderate and (c) Extensive damage states under mainshock.....	27
Figure 5.2	Conditional time-dependent limit-state occurrence probabilities in the post-mainshock environment for the Era 11 bridge in the (a) Intact; (b) Slight; and (c) moderate damage states immediately following the mainshock.	30
Figure 5.3	Comparing the time-dependent mainshock-only and mainshock-aftershock occurrence probabilities for the (a) Slight and (b) Complete limit states for all three bridges.....	31

1 Introduction

Bridges are an essential part of transportation systems, and the mobility of emergency responders in the event of a seismic event is highly dependent on a functioning transportation network. Determination of the structural integrity and functionality of earthquake-damaged bridges is a critical part of post-event response and recovery. Due to their high rate of occurrence within a short time window after the causative mainshock, aftershocks could further hamper the functional restoration of bridges and, in addition, threaten their structural integrity after their lateral load-carrying capacity is reduced under the mainshock.

Currently, the California Department of Transportation (Caltrans) uses a set of system-level damage states as the basis for classifying the post-earthquake operability of bridges. The damage states are based on HAZUS [FEMA 2012] classifications (minor, moderate, extensive, and complete), and each one is assigned a “likely post-event traffic state” [Mangalathu et al. 2016; Mangalathu 2017]. Despite HAZUS being the primary tool used as the basis for post-earthquake decisions regarding the partial or complete closure of bridges, the extent to which knowledge of residual structural capacity and time-dependent aftershock hazard and risk, and how these factors inform these damage-traffic-state relationships is unclear.

Although significant advances have been made in estimating bridge seismic vulnerability and risk under mainshock events (e.g., Mackie and Stojadinovic [2001]; Nielson [2005]; Mackie and Stojadinović [2006]; Banerjee and Shinozuka [2008]; Zhang et al. [2008]; Vosooghi and Saiidi [2010] Ramanathan [2012]; Mangalathu et al. [2017]; Soleimani et al. [2017]; Mangalathu and Jeon [2018]; and Mangalathu et al. [2018]), research to quantify the time-dependent vulnerability and risk in the aftershock environment is still in its infancy. A few studies have been carried out to estimate the vulnerability of bridges that have been damaged by mainshocks [Franchin and Pinto 2009; Alessandri et al. 2013; Ghosh et al. 2015; Jeon et al. 2016; and Omranian et al. 2018].

Franchin and Pinto [2009] suggested an approach to determine when to open or close mainshock-damaged bridges in the presence of aftershock hazard by estimating the transition probability from a mainshock damage state to collapse state. The authors combined mainshock and aftershock fragilities with probabilistic seismic hazard analysis (PSHA) to assess the collapse risk, which was used as the basis for closure decisions; this methodology was applied in a case study of a viaduct bridge in Italy.

Alessandri et al. [2013] proposed a methodology for evaluating the feasibility of continuing bridge operations after a mainshock while accounting for the effect of aftershocks. The damage state of the bridge following the mainshock is estimated by combining the analytical fragility curves with information gleaned from *in situ* visual inspections. The authors proposed usability criteria for the bridge based on the expected aftershock risk. For California bridges, Jeon et al. [2016] investigated the effect of successive earthquakes on mainshock-damaged bridges. The study concluded that the additional damage to columns caused by aftershocks is more pronounced when the bridge undergoes higher mainshock damage states. The authors also evaluated the effect of various retrofitting strategies for mitigating aftershock vulnerability.

Recently, Omranian et al. [2018] investigated the effect of skew angle and ground-motion orientation on the fragility curves of skewed bridges under mainshocks and aftershocks. The study revealed that the skew angle and angle of incidence have a significant influence on the aftershock fragility curves of a California bridge. Note, to date the aftershock studies for bridges in California have been limited to two-span bent bridges, and there have been no investigations on the effect of time-dependent aftershock hazard on the seismic risk. As noted in Mangalathu [2017], single-column bent bridges occupy a significant portion of the California inventory. Although several studies have highlighted the time-dependent nature of seismic hazard in the post-mainshock environment and its impact on the seismic risk evolution for buildings, none have been conducted on the time-dependent seismic risk of typical California bridges in the post-mainshock environment. The specific objectives of the research reported herein was as follows:

1. Select mainshock and aftershock ground motions for single-site time-dependent risk assessment of California bridges.
2. Investigate the seismic risk in California highway bridges under mainshock-aftershock sequences using sequential nonlinear response history analyses (RHAs). The first ground motion in the sequence will be used to induce a specified level of damage in the structure, and the second will be used to evaluate the response of the mainshock-damaged bridge. Post-mainshock states ranging from intact to imminent collapse are considered. These states will be used to define the possible damaged condition of the bridge after being subjected to mainshock or aftershock ground motions. The results from nonlinear RHAs will be used to populate the elements of a set of Markov transition matrices. These Markov matrices are central to the time-dependent bridge seismic risk analysis.
3. Explore the effect of construction era on the time-dependent seismic risk of California bridges, which can be grouped into three categories based on the adopted design philosophy: constructed before 1971 (Era 11, hereafter), constructed between 1971 through 1990 (Era 22, hereafter) and constructed after 1990 (Era 33, hereafter). To date, no studies have been carried out on the effect of these design eras on aftershock risk for bridges located in California .

The report is organized as follows: Chapter 2 outlines the ground-motion selection for mainshock and aftershock performance assessment. The seismic hazard evaluation (mainshock and aftershock) of a selected site in California is also presented. Chapter 3 outlines the proposed framework, and the nonlinear structural modeling approach is presented in Chapter 4. The results from the seismic risk evaluation are detailed in Chapter 5.

2 Ground-Motion Selection and Probabilistic Seismic Hazard Analysis

2.1 INTRODUCTION

The best way to obtain reasonable estimates of a structure’s seismic response is to perform nonlinear RHAs using a representative set of ground motions based on the site of interest. The objective of the current study is to evaluate the seismic performance of individual bridges when they are subjected to a major mainshock event and subsequent aftershocks. As such, it is necessary to first recognize the likely differences in the attributes of mainshock and aftershock ground motions, and then select a representative group of record pairs.

Significant differences in the frequency content of mainshock and aftershock ground motions have been reported in literature (Chiou and Youngs [2008]; Ruiz-García and Negrete-Manriquez [2011]; and Abrahamson et al. [2013]). Several factors affect the characteristics of aftershock ground motions. Aftershocks are generally smaller in magnitude [Shcherbakov and Turcotte 2004] and, for the same site, have larger source-to-site distances (possibly as a result of having a smaller rupture area) than their causative mainshocks. Second, even when source and path differences are considered, there is evidence of a mild correlation between the characteristics of mainshock and aftershock records belonging to the same sequence [Boore et al. 2014]. Selecting mainshock-aftershock (MS–AS) record pairs from the same sequence is considered “ideal” because the inherent relationship between the sequential ground motions will be explicitly captured. When considering other constraints that might arise in selecting ground motions for sequential RHAs (e.g., matching target magnitude (M), distance (R), and V_{s30} to target a specific ε value from hazard deaggregation), it may not be possible to find an adequate number of record pairs from the same sequence. Selection of MS–AS record pairs that do not necessarily belong to the same sequence or pairs of mainshock-only records (which are usually much more readily available compared to aftershock records) would allow access to a broader pool of ground motions, which has obvious benefits, but at the cost of possibly not preserving the within-sequence ground-motion correlations [Boore et al. 2014].

A few studies have investigated differences in the dynamic response of structures subjected to mainshock-mainshock (MS–MS) versus MS–AS ground-motion sequences. Goda [2012] compared the ductility demands imposed by MS–MS and MS–AS sequences. The MS–

MS sequences were selected such that the distribution of the magnitudes of the events producing the second motion in the pair would match the aftershock magnitude distribution predicted by Omori's law [Utsu et al. 1995]; the effects of different rupture distances were not considered. A third foreshock–MS–MS sequence was also considered (originally proposed by Hatzigeorgiou and Beskos [2009]) in which the foreshock and aftershock records are scaled versions of the mainshock records (by a factor of 0.85). The probability distribution of the peak ductility demands developed for a set of single-degree-of-freedom (SDOF) structures with different periods showed slight differences between responses obtained from the MS–AS record pairs and the MS–MS sequences generated based on Omori's law; the triad sequence produced significantly higher peak ductility demands. In a separate study, Goda [2015] compared the collapse performance of a two-story wood-frame building under both MS–MS and MS–AS ground-motion pairs. In contrast to the earlier study [Goda 2012], the MS–MS sequence used the same records in the second event as in the first. Not surprisingly, the MS–MS sequence produced higher collapse probabilities than the one with MS–AS records. Ruiz-García [2012] conducted a similar study considering two low- and mid-rise steel frames, and reached the same conclusion.

The difference in the frequency content of mainshock and aftershock ground motions has also been investigated in the development of recent ground-motion models (GMMs). Using a systematic approach to compare ground motions that allows for controlling for source and site characteristics (e.g., \mathbf{M} and R), Boore et al. [2014] examined the correlation of event terms from parent mainshocks and their children aftershocks using the PEER NGA-West 2 database [Chiou et al. 2008]. A mild correlation between the event terms was observed. No adjustment for aftershocks was included in the final functional form of their GMM as the difference between the event terms of mainshocks and average of event terms from aftershocks was practically zero and independent of magnitude. For the original NGA project [Chiou et al. 2008], functional forms used in some of the GMMs included a term to distinguish mainshocks from aftershocks. Abrahamson et al. [2013] found that the median spectral values of aftershocks at short periods were smaller than those from similar mainshocks, whereas the aftershock spectral ordinates were larger at longer periods (> 0.75 sec).

As shown in Figure 2.1, Chiou and Youngs [2008] reached a similar conclusion, but the transition from lower to higher spectral ordinates (of aftershocks relative to mainshocks) was about 2.0 sec. Such a relationship between S_a values of mainshocks and aftershocks needs to be viewed in the context of the different \mathbf{M} and R expected for these two event types. Whereas aftershock demands will generally be smaller (due to lower \mathbf{M} and larger R), their spectral shape is different from that of mainshocks; see Figure 2.1. Chiou and Youngs also found that the style of faulting for aftershocks had a smaller influence on the predicted spectral values when compared to mainshocks, but the depth to top of rupture (Z_{TOR}) had a stronger influence on the predictions made for aftershocks.

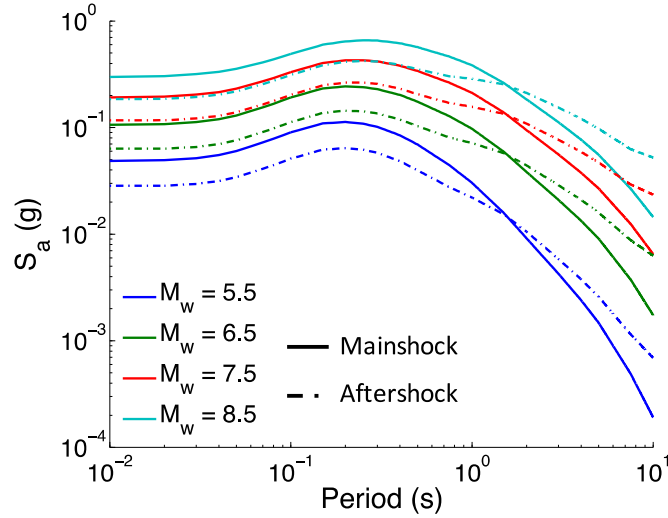


Figure 2.1 Comparing the spectra of mainshock and aftershock records with similar magnitudes obtained from the Chiou and Youngs [2008] GMM.

2.2 RECORD PAIRS FOR RESPONSE HISTORY ANALYSIS

Given the previously mentioned measurable differences in the frequency content of mainshock and aftershock ground motions and their implications for RHA, the mainshock–aftershock record pairs in this study are selected from ground motions that are specifically identified through the use of time and distance windowing algorithms, as the actual seismic sequences of major earthquakes [Knopoff and Gardner 1972; Wooddell and Abrahamson 2014]. The ground-motion pairs are from the Class 1 (mainshock) and Class 2 (aftershock) records of the Imperial Valley 06, Northridge, Livermore, Coalinga, Landers, Mammoth Lake, Chalfant Valley, Whittier Narrows, Darfield, Umbria Marche, and Chi-Chi earthquakes, which are available in the PEER-NGA-West2 database [Chiou et al. 2008]. A magnitude-dependent time window and a distance threshold of 40 km measured in terms of the centroidal Joyner–Boore distance [Wooddell and Abrahamson 2014] was used to identify the aftershock ground motions. The magnitudes of the events that produced the selected ground motions range from 5.80 and 7.62 for mainshocks, and 5.01 and 6.46 for aftershocks. Pulse-like ground motions were excluded from the set of 34 record pairs. Table 2.1 summarizes the properties of the records in each ground-motion sequence. The response spectra of the mainshock and aftershock ground motions are shown in Figures 2.2 and 2.3, respectively.

Table 2.1 Attributes of the mainshock-aftershock ground-motion sequences.

Sequence ID	Event name	Mainshock ground motion			Aftershock ground motion		
		M_w	R (km)	V_{s30} (m/sec ²)	M_w	R (km)	V_{s30} (m/sec ²)
1	Imperial Valley 06	6.53	22	242	5.01	24	237
2	Northridge	6.69	12	546	5.20	20	508
3	Northridge	6.69	9	356	5.93	22	450
4	Northridge	6.69	20	450	5.28	18	379
5	Northridge	6.69	10	706	5.28	14	409
6	Livermore	5.80	15	378	5.42	28	517
7	Coalinga	6.36	24	275	5.09	24	467
8	Landers	7.28	24	354	6.46	35	297
9	Mammoth Lakes 01	6.06	13	537	5.69	14	537
10	Chalfant Valley 02	6.19	22	371	5.44	24	303
11	Whittier Narrows	5.99	10	267	5.27	22	316
12	Whittier Narrows	5.99	20	321	5.27	24	297
13	Whittier Narrows	5.99	15	371	5.27	23	271
14	Whittier Narrows	5.99	18	301	5.27	21	347
15	Whittier Narrows	5.99	11	329	5.27	17	325
16	Whittier Narrows	5.99	17	241	5.27	19	345
17	Whittier Narrows	5.99	25	303	5.27	34	318
18	Whittier Narrows	5.99	19	412	5.27	29	400
19	Whittier Narrows	5.99	7	969	5.27	17	371
20	Whittier Narrows	5.99	0	401	5.27	12	545
21	Umbria Marche	6.00	19	401	5.50	36	492
22	Darfield	7.00	44	638	6.20	85	638
23	Darfield	7.00	31	255	6.20	67	561
24	Darfield	7.00	52	551	6.20	62	484
25	Chi-Chi	7.62	33	348	6.20	36	379
26	Chi-Chi	7.62	19	492	6.20	23	543
27	Chi-Chi	7.62	39	573	6.20	41	492
28	Chi-Chi	7.62	83	250	6.20	91	541
29	Chi-Chi	7.62	53	789	6.20	60	573
30	Chi-Chi	7.62	47	453	6.20	51	278
31	Chi-Chi	7.62	48	438	6.20	53	573
32	Chi-Chi	7.62	50	614	6.20	92	411
33	Chi-Chi	7.62	60	484	6.20	77	573
34	Chi-Chi	7.62	82	496	6.20	97	489

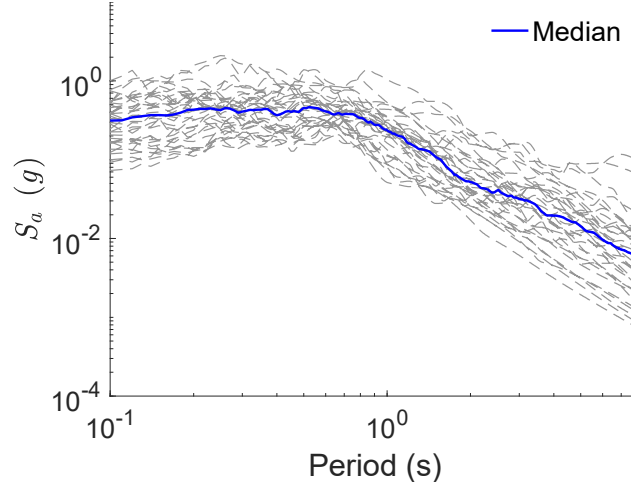


Figure 2.2 Individual and median response spectra for the mainshock ground motions.

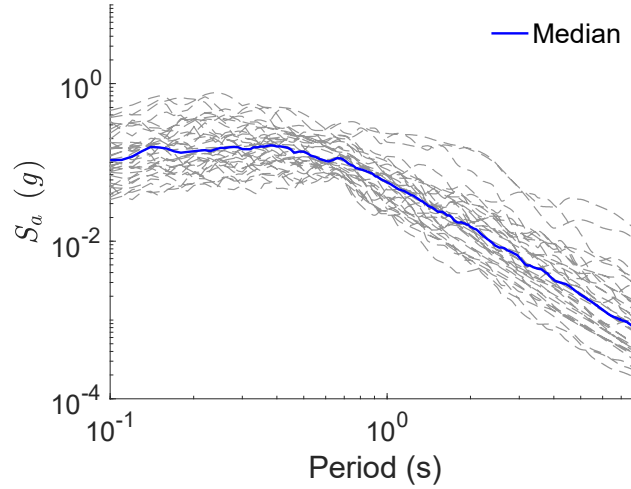


Figure 2.3 Individual and median response spectra of aftershock ground motions.

The intensity measure (IM) used to represent and scale the ground motions is their 5%-damped spectral acceleration at a period of 1 sec. Numerous prior studies have been dedicated to proposing ground-motion selection guidelines for use in nonlinear dynamic analysis, e.g., Kalkan and Chopra [2010] and ATC [2017]. These guidelines have mostly been focused on the selection criteria that would result in a less-disperse and unbiased estimate of the seismic performance of the structure being examined while minimizing the computational effort associated with the nonlinear dynamic analysis. While there are conflicting recommendations in terms of the impact of (M) , (R) , and V_{s30} of ground motions without forward-directivity effects on the outcomes of nonlinear dynamic analysis [Bommer and Acevedo 2004; Shome et al. 1998], the spectral shape parameter (ε) of a ground motion is often recognized as the parameter that has the most significant effect on structural performance [Baker and Cornell 2006; Haselton et al. 2009]. Prior studies of earthquakes that occur in California have suggested that ground motions with long return periods usually have a peaked spectral shape, with a positive ε value that ranges between 1

and 2 [Haselton et al. 2009]. If the ground motion set used in RHA is selected without properly accounting for this peaked spectral shape, the seismic performance of the examined structure could be significantly underestimated.

To ensure that the spectral shape of the ground motions used in the RHAs reflect the site of interest, the 34 record pairs were selected such that their ε values would match the ε value of the location of the bridges obtained from seismic hazard deaggregation [Bazzurro and Cornell 1999].

2.3 PROBABILISTIC SEISMIC HAZARD ANALYSIS

To develop mainshock hazard curves, conventional PSHA [Kramer et al. 1996] is performed while the aftershock hazard curves are generated using the approach suggested by Yeo and Cornell [2009]. Probabilistic seismic hazard analysis and aftershock PSHA (APSHA) are performed using source and magnitude models that are simpler than the USGS models but still account for all the sources that contribute to the seismic hazard at the site of interest. Seismic hazard analyses were performed for a high seismicity site in Southern California (33.996, -118.162). The parameters that define the spatial distribution of the earthquake magnitudes and the time-dependent aftershock rate are adopted from the California model suggested by Reasenber and Jones [1989]. The Boore and Atkinson [2008] ground-motion prediction equation (GMPE) was used to obtain the statistical distribution of the IM conditioned on the magnitude and distance.

Following the work of Ramanathan [2012], the spectral acceleration at a period of one second, $Sa_{1.0s}$, is adopted as the IM. The magnitude of the largest aftershock is assumed to be equal to that of the largest mainshock. The minimum magnitude is taken as 5 as events with smaller magnitudes are not likely to induce notable damage in bridge structures. The relationship that forms the basis of conventional (mainshock) PSHA is shown in Equation (2.1). v_i is the rate of occurrence of seismic events with magnitudes larger than 5.0 for source i and $G(IM > im | M, R, \varepsilon)$ is an indicator function whose value is 1.0 if $IM > im$ and 0.0 otherwise. When performing APSHA, v_i is replaced with μ_{AS} for each time interval k from Equation (3.4).

$$\lambda_{IM}(IM > im) = \sum_{i=1}^{N_{AS}} v_i \iiint_{M,R,\varepsilon} G(IM > im | M, R, \varepsilon) f_M(m) f_R(r) f_\varepsilon(\varepsilon) dM dr d\varepsilon \quad (2.1)$$

The mainshock hazard curve shown in Figure 2.4 is developed for all faults contributing to the total seismic hazard at the site, whereas the aftershock hazard curve is only for the single fault that is the primary source of mainshock hazard at the assumed location. The APSHA hazard curve is limited to a single fault because the concurrent occurrence of multiple mainshocks that would trigger aftershocks on different faults is unlikely. The APSHA hazard curve is developed for a time window of one year starting immediately after the occurrence of the mainshock. A

quick comparison between the PSHA and APSHA hazard curves in Figure 2.4 reveals substantially higher aftershock hazard compared to the mainshock hazard.

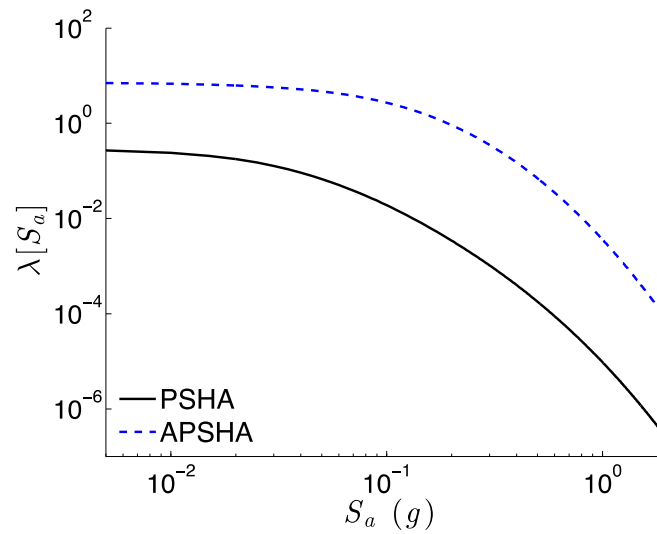


Figure 2.4 Mainshock and aftershock (for 1 year after the occurrence of the mainshock) seismic hazard curves for $T = 1.0$ sec.

3 Markov-Based Risk Assessment Framework

The current version of the performance-based earthquake engineering (PBEE) framework assumes that the state of a structure prior to the occurrence of a seismic event is known (usually the structure is assumed to be in the intact state), and the structure will always return to its intact state before the next earthquake occurs. When performing seismic risk analysis under major mainshock events, this is a reasonable assumption as the time interval between major mainshock events is usually long enough to allow for affected structures to be restored to their intact state.

In the post-mainshock environment, structures that have sustained some level of structural damage are usually not repaired during the short time period immediately following the mainshock when the rate of occurrence of aftershocks is highest. This, coupled with the accumulation of structural damage under multiple post-mainshock events, adds to the uncertainty in determining the state of a structure before being subjected to each subsequent aftershock. As such, evaluating the seismic performance of structures subjected to sequential seismic events requires explicit consideration of the uncertainty in the state of the structure after being subjected to any of the events in a cluster comprising a mainshock and subsequent aftershocks.

The probability of a bridge transitioning from one damage state to the next can be evaluated using a Markov process [Yeo and Cornell 2009]. A key assumption in the Markov process is that the state of the bridge under event i in the sequence is dependent only on its state under the event $i-1$, and is independent of its states under the events that precede event $i-1$. The uncertainty in the state of the bridge is considered through the Markov transition matrix [Equation (3.1)], whose elements represent the probability of transitioning between the r pre-defined limit states.

$$\Pi = \begin{bmatrix} P_{11} & P_{12} & \cdots & P_{1r} \\ 0 & P_{12} & \cdots & P_{2r} \\ \vdots & \vdots & \ddots & \vdots \\ 0 & 0 & \cdots & P_{rr} \end{bmatrix} \quad (3.1)$$

P_{ij} in Equation (3.1) is the probability that the bridge transitions from damage state i (in response to the previous event) to damage state j when subjected to a new event. The Markov

transition matrix (Π) has an upper triangular form since no repair measures are assumed to have taken place to restore the bridge to a less severe damage state. Diagonal elements in Equation (3.1) represent a “no-limit-state-transition” when the bridge is subjected to a seismic event.

To calculate the $p_{ij}, j > i$ terms of the transition matrix Π in Equation (3.1) during a time window (t_0, t_m) where t_0 is measured from the occurrence of the causative mainshock, the time window can be broken into small intervals such that the probability of occurrence of more than one aftershock during each interval is negligible. With this assumption, the P_{ij} terms for a single seismic source in each interval (t_{m-1}, t_m) of the time window (t_0, t_1) can be calculated:

$$P_{ij}(t_{m-1}, t_m) = P(N_{AS} = 1) \int \left[P_{ij}^{DS}(EDP > edp_j | IM) - P_{i,j+1}^{DS}(EDP > edp_{j+1} | IM) \right] f_{IM}(im) d im \quad (3.2)$$

where $P(N_{AS} = 1)$ is the probability of occurrence for a single aftershock during each time interval (t_{m-1}, t_m) , and $P_{ij}^{DS}(EDP > edp_j | IM) - P_{i,j+1}^{DS}(EDP > edp_{j+1} | IM)$ is the probability that the bridge would experience damage state j under the current seismic event given that it has already sustained damage state i when subjected to the preceding seismic event. $f_{IM}(im)$ is the source-specific probability density function of the intensity measure (IM) that links the response of the bridge to the seismic hazard at its location and can be obtained through PSHA.

It is usually assumed that the occurrence of seismic events can be characterized with a Poisson distribution. As such, $P(N_{AS} = 1)$ in Equation (3.2) can be calculated using Equation (3.3), where the mean rate of aftershocks during the time interval (t_{m-1}, t_m) [$\mu_{AS}(t_{m-1}, t_m)$] can be obtained using Equation (3.4). More specifically, Equation (3.4) is used to calculate the mean number of aftershocks on a seismic source with minimum and maximum magnitudes of M_0 and M_m , and is obtained by combining the modified Omori’s law for the daily rate of aftershocks and Gutenberg-Richter’s relationship for the magnitude distribution [Reasenber and Jones 1989; Yeo and Cornell 2009]; M_m is usually taken as the mainshock’s magnitude. a and b are constants that characterize the magnitude distribution and c and ρ are constants that define the temporal decay in the number of aftershocks.

$$P_2(N_{AS} = 1) = \mu_{AS}(t_{m-1}, t_m) e^{-\mu_{AS}(t_{m-1}, t_m)} \quad (3.3)$$

$$\mu_{AS}(t_{m-1}, t_m) = \left[10^{a+b(M_m-M_0)} - 10^a \right] \frac{(t_m + c)^{1-p} - (t_{m-1} + c)^{1-p}}{1-p} \quad (3.4)$$

The decline in aftershock seismic hazard with the elapsed time since the occurrence of the mainshock [Utsu et al. 1995] means that the Markov transition matrix of Equation (3.1) will be non-stationary, with elements that can be calculated through Equation (3.5).

$$\Pi(t_{m-1}, t_m) = \begin{bmatrix} P_{11}(t_{m-1}, t_m) & P_{12}(t_{m-1}, t_m) & \cdots & P_{1r}(t_{m-1}, t_m) \\ 0 & P_{22}(t_{m-1}, t_m) & \cdots & P_{2r}(t_{m-1}, t_m) \\ \vdots & & \ddots & \vdots \\ 0 & 0 & \cdots & 1 \end{bmatrix} \quad (3.5)$$

At time step k after the occurrence of the mainshock, the cumulative probability that the structure is in damage state j —given that it has undergone damage state i under the mainshock—is equal to the element on row i and column j of matrix P^k in Equation (3.6).

$$P^k = \Pi_{m=1}^k \Pi(t_{m-1}, t_m) \quad (3.6)$$

Equations (3.1) through (3.6) provide a probabilistic framework to assess the seismic performance of bridges in the post-mainshock environment. The framework can be easily extended to perform seismic risk assessment due to sequential events in the pre-mainshock environment following the same logic and steps mentioned earlier in this section.

Unlike the post-mainshock risk evaluation, the pre-mainshock environment considers the uncertainty in the occurrence of the mainshock and associated damage to the structure. This uncertainty can be incorporated into the Markov process by multiplying the aftershock limit state transition matrix in Equation (3.6) by a vector of p_i^{MS} values as shown in Equation (3.7). The vector of $\lambda_{i,n}^{MS}$ values represents the mean annual rate of the structure experiencing damage state i , $i = 1, \dots, r$ under the mainshock ground motions. The summation in Equation (3.7) accounts for all the seismic sources (N_s) that contribute to the seismic hazard at the site of interest.

$$\lambda_{PreMS}^m = \sum_{n=1}^{N_s} \left[\left(\lambda_{1,n}^{MS}, \dots, \lambda_{r,n}^{MS} \right) \Pi_{m=1}^k \Pi_n(t_{m-1}, t_m) \right] \quad (3.7)$$

Each element of the λ_{PreMS}^m vector obtained from Equation (3.7) can be used as the input for a Poisson (or exponential) distribution to calculate the limit state exceedance probabilities over any desired time window.

As shown in Equation (3.8), the $\lambda_{i,n}^{MS}$ terms can be obtained by subjecting the bridge to mainshock ground motions to induce the desired target level damage $\left[P_{MS}^{DS}(EDP > edp_i | IM) - P_{MS}^{DS}(EDP > edp_{i+1} | IM) \right]$, where λ_{IM}^n is the mean annual frequency of exceedance of the IM and can be obtained through mainshock seismic hazard analysis.

$$\lambda_{i,n}^{MS} = \int \left[P_{MS}^{DS}(EDP > edp_i | IM) - P_{MS}^{DS}(EDP > edp_{i+1} | IM) \right] d\lambda_{IM}^n(im) \quad (3.8)$$

|

4 Bridge Nonlinear Structural Modeling and Limit State Definitions

4.1 INTRODUCTION

The aftershock risk assessment framework presented in Chapter 2 is implemented on a set of two-span single-column bent bridges with seat abutments. Two-span box-girder bridges make up a significant portion of California bridge inventory [Mangalathu 2017], and three bridges from different design eras (Era 11, Era 22 and Era 33) were considered.

4.2 NUMERICAL MODELING

The following section presents the modeling considerations for various bridge components, which can generally be categorized based on whether they are located in the superstructure or substructure. The superstructure (bridge deck) typically remains elastic during an earthquake and is therefore modeled using elastic beam–column elements; see Figure 4.1.

4.2.1 Substructure

4.2.1.1 Bents

The bents are modeled using a combination of displacement-based beam–column elements and rigid links to facilitate moment and force transfer between the members of the bent. The finite-element discretization of a single column bent is shown in Figure 4.2.

4.2.1.2 Columns

Columns are one of the most seismically vulnerable components in a bridge. In fact, most of the past earthquake-induced bridge failures have been attributed to column damage. Displacement-based beam–column elements with fiber-defined cross sections were used to model the columns; see Figure 4.2. Fiber cross sections have the distinct advantage of incorporating unique material properties for different locations across a member’s cross section. For instance, confined concrete is used to represent the concrete behavior in the core section of the column, while unconfined concrete is used to represent the unconfined cover concrete. The Chang and Mander [1994] model is used to define the monotonic stress–strain curves of confined and unconfined concrete.

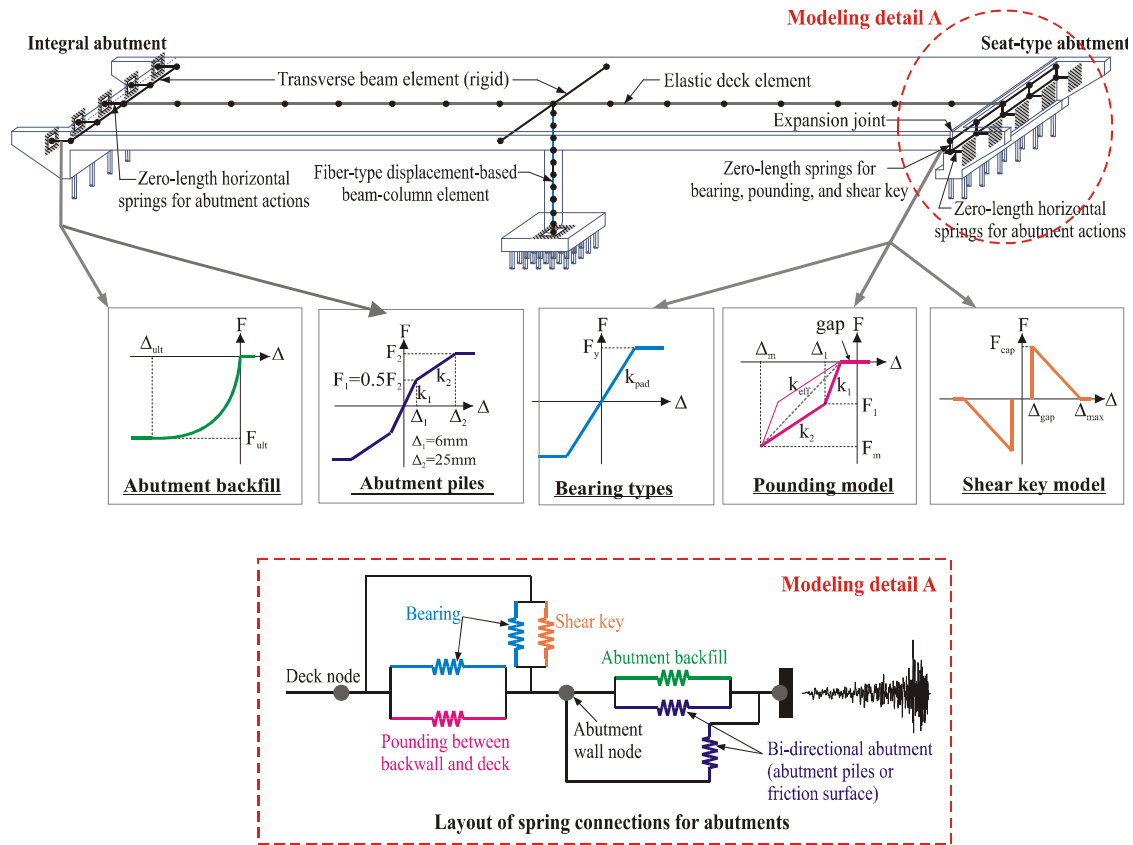


Figure 4.1 Numerical modeling of various bridge components.

4.2.1.3 Abutments

Abutments can be classified into two basic types: diaphragm abutments and seat abutments [Ramanathan 2012]. Diaphragm abutments are cast as being monolithic with the superstructure. As they engage the backfill soil during seismic action, they provide a good source of energy dissipation and reduce the likelihood of span unseating. Seat abutments provide a bearing support to the superstructure, which is restrained longitudinally by the abutment backwall and transversely by the piles and the shear key. When the deck is in contact with the abutment backwall in the longitudinal direction, the bridge's stiffness and resistance to seismic action increases. As the superstructure moves away from the abutment, the primary resistance comes from the bearing pads, making it susceptible to unseating. The backwall of the seat abutment is typically designed to fail under impact and passive response before damaging forces are transmitted to the lower portion of the abutment.

Abutment response to seismic loading is dependent on pressure from the earthquake and the structure. The pressure of soil on the abutment is due to the longitudinal response of the bridge deck and includes passive and active resistance. Passive resistance is provided by the friction between the backfill soil and pile surface (depending on the abutment footing type). It develops when the abutment moves toward the backfill soil. These frictional forces contribute to

the active resistance, which is activated when the abutment moves away from the backwall soil. The passive response of the abutment backwall is simulated using the hyperbolic soil model proposed by Shamsabadi and Yan [2008]. The model is based on experimental testing of bridge abutments conducted at the University of California Los Angeles with 5.5-ft-high backwalls and typical non-cohesive and cohesive backfill soils. The test results were then extended to develop closed-form solutions for the abutment backfill soil response for a range of backwall heights based on a series of analyses using the limit-equilibrium method that implements mobilized logarithmic-spiral failure surfaces coupled with a modified hyperbolic soil stress-strain behavior.

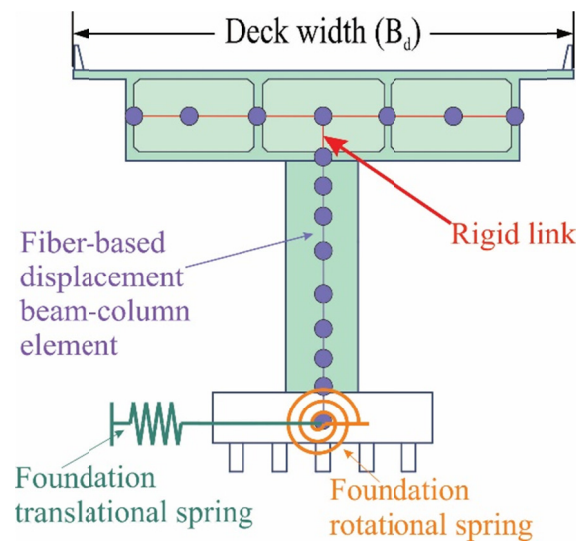


Figure 4.2 Finite-element discretization of a single-column bent.

4.2.1.4 Abutment Piles

Abutment piles provide longitudinal and transverse stiffness to the abutments. The trilinear force-deformation response of the pile, along with the associated modeling parameters, are presented in Figure 4.1. The initial yield parameters (Δ_1 , F_1) are determined based on the design recommendations of the Caltrans 2014 draft of bridge design aids on *Permissible Horizontal Loads for Standard Plan and Steel HP Piles* [Mangalathu 2017]. The plastic yielding parameters (Δ_2 , F_2) are calculated based on the results from modeling various pile systems simulated in LPILE [Mangalathu 2017]. The pile hysteretic behavior is captured using the *Hysteretic* material in OpenSees with the hysteretic parameters *pinchX* and *pinchY* set to 0.75 and 0.5, respectively [Ramanathan 2012].

4.2.1.5 Elastomeric Bearings

Elastomeric bearings decouple the superstructure from the substructure, which makes the superstructure susceptible to large deformations. The elastomeric bearing is assumed to be elasto-plastic, and the yield force, F_y , is obtained by multiplying the normal force by the

coefficient of friction. The force-deformation response of the elastomeric bearing is shown in Figure 4.1.

4.2.1.6 Shear Keys

Shear keys help restrain the relative transverse movement between the deck and the bridge abutments. Earthquake-induced shear key can result from one of four mechanisms: shear friction, flexure, shear, and bearing [Megally et al. 2002]. The shear-key designs are categorized as isolated (emerging designs) or non-isolated (conventional designs) [Mangalathu 2017]. Since the isolated shear key is a new type of design and does not exist in the current inventory, this study will only focus on the non-isolated shear keys. The nonlinear model of the shear key is depicted in Figure 4.3. F_{cap} denotes the capacity of the shear key, which is computed as the product of the dead-load reaction and the acceleration [Caltrans 2012]. Megally et al. [2002] conducted a series of experiments on shear keys and found that $\Delta_{max} - \Delta_{gap}$ equal to 3.5 in. is the deformation at which the capacity of the shear key essentially degrades to zero.

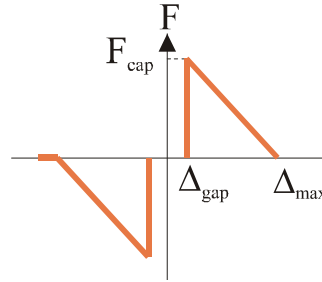


Figure 4.3 Shear key model.

4.2.1.7 Pounding

Seismic pounding refers to impact between bridge decks, between the deck and the abutment, or between the adjacent decks in a multi-frame bridge in the longitudinal direction. Impact occurs when the relative displacement between adjacent decks or the deck and the abutment exceeds the gap separating them. Significant pounding damage was observed at the I-5/SR-14 interchange during the 1994 Northridge, California, earthquake [Muthukumar and DesRoches 2006]. The contact element developed by Muthukumar and DesRoches [2006] was used to model the pounding between the superstructure and abutments. This material model explicitly accounts for the loss of hysteretic energy; see Figure 4.4. The maximum deformation, Δ_m , is assumed to be 1.0 in. The yield deformation, Δ_1 , is assumed to be $0.10\Delta_m$. The stiffnesses, k_1 and k_2 , are recommended to be 1022.3 kip/in./ft and 351.755 kip/in./ft, respectively.

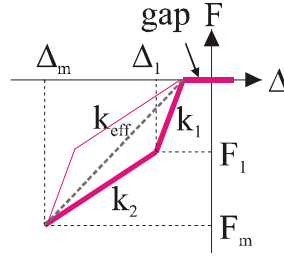


Figure 4.4 Analytical model of pounding between the deck and abutment back wall.

4.2.1.8 Foundation

The foundation transmits service and ultimate loads from the structure to the underlying soil. Foundations can be classified as either shallow or deep. As the name implies, for shallow foundations, the loads from the structure are transferred to the underlying soil at shallow depths. Deep foundations (piles) are used when soil conditions are not favourable to shallow foundations. The type of bridge foundation is determined based on various factors, e.g., the condition of the soil, overhead clearance, existing utilities, and proximity to existing facilities such as buildings and railroads [Mangalathu 2017]. For the bridges considered in the current study, foundations are modeled using elastic translational and rotational springs placed at the base of the column.

The numerical models for the various components are integrated to produce a global analytical model of the bridge. Displacement-based beam-column elements are used to model the columns. Translational and rotational springs are added to the base of the column to simulate the behavior of the footing. Zero-length elements capturing the response of the abutment backfill soil under bi-directional loading (abutment piles or frictional surface) are connected in parallel and to the transverse deck elements in the case of diaphragm abutments. Bearing-pad elements and pounding elements are also modeled with zero-length springs and are connected in parallel to the abutment springs in the case of seat abutments.

4.3 CASE STUDY BRIDGE CONFIGURATIONS

Figure 4.5 shows the details of the selected bridge and the associated geometric properties. The bridge has a deck width of 9.9 m with a span length of 30.5 m, and is supported by seat abutments with cast-in drilled concrete piles (with stiffness per deck width of 116 kN/m). The abutments are 7.5 m high, and elastomeric bearings are used to support the superstructure. Following the work of Mangalathu [2017], the coefficient of friction and stiffness of the bearing per deck are estimated as 0.30 and 1060 N/mm/m, respectively. The diameter of the column is 1524 mm with a longitudinal reinforcement ratio of 0.02 (36 No. 11 bars). The transverse reinforcement in the Era 11 bridge includes No.5 bars with a pitch of 300 mm. In Era 22 and Era 33, the spacing of the transverse reinforcement is 90 mm and 75 mm, respectively.

The concrete compressive strength in the superstructure and column is 33.0 MPa, and the yield strength of the reinforcement is 465 MPa. The mass density of the concrete and damping

ratio is assumed as to be 2400 kg/m^3 and 4.5% , respectively. The translational and rotational stiffness of the foundation is 300 kN/mm and $4.5 \times 10^9 \text{ N-m/rad}$. For the Era 11 bridge, the gap between the abutments and the deck is 21 mm . For the same bridge, the gap between the shear key and the superstructure is 12.5 mm . The shear keys at the abutments are designed to resist a force of $1g$ times the superstructure dead-load reaction at the abutments. Interested readers are directed to Mangalathu [2017] for an evaluation of the stiffness and strength properties of various bridge components.

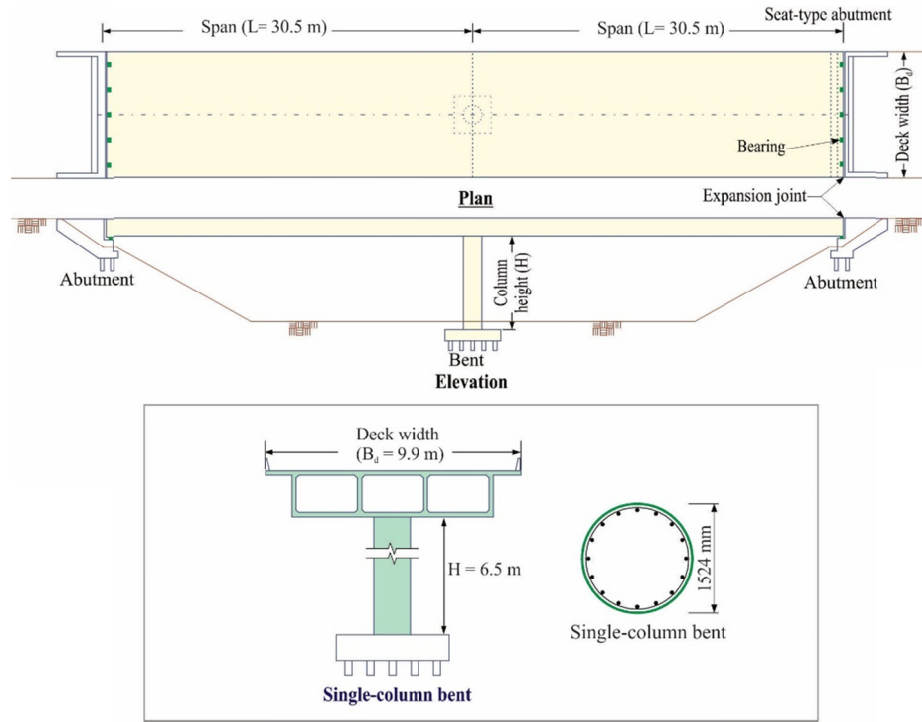


Figure 4.5 Schematic illustration of the bridge layout.

4.4 LIMIT STATES: DEFINITIONS

The description of the bridge column limit states are provided in Table 4.1. The column curvature ductility, which is used to link response demands to the physical damage descriptions, is assumed to follow a lognormal distribution with the median values and dispersions shown in Table 4.1. The dispersion, β , is taken as a constant (0.35) for all eras [Ramanathan 2012; Mangalathu et al. 2016; Jeon et al. 2016; and Mangalathu 2017].

Table 4.1 Limit state descriptions for bridge columns [Mangalathu 2017].

Limit state	Column state	Column damage	Column repair	Column curvature ductility			
				Median value			Dispersion (β)
				Era 11	Era 22	Era 33	
Slight	None or aesthetic	EQ-related minor cracking	Seal and paint	0.8	1.0	1.0	0.35
Moderate	Minor repairs needed	Minor spalling of cover concrete	Epoxy inject, minor removal/patch	2.0	5.0	5.0	0.35
Extensive	Major repairs needed, but function intact	Exposed core, confinement yield	Major removal/patch. Add jacket.	5.0	8.0	11.0	0.35
Complete	Irreparable damage, function compromised	Bar buckling, large drift, core crushing	Remove/Replace column (or bridge)	8.0	11.0	17.0	0.35

5 Demonstration of the Proposed Framework

5.1 MAINSHOCK AND AFTERSHOCK FRAGILITY CURVES

Incremental dynamic analyses are performed on the bridge structural models, and the response demands are used to develop fragility curves. The demand at each IM is convolved with the capacity estimates to compute the probability of limit state exceedance at that IM. The fragility curve parameters (median and log-standard-deviation) are then obtained by applying the maximum likelihood method [Baker 2015]. The aftershock fragility curves are generated by performing sequential nonlinear RHAs, where the bridge models are subjected to the mainshock-then-aftershock ground motions. Within this sequence, the mainshock ground motions are scaled to target specific damage levels: Slight, Moderate, and Extensive as described in Table 5.1.

Figure 5.1 shows how the probability of exceedance for the Complete limit state is affected by mainshock damage. More specifically, Figure 5.1(a), 5.1(b), and 5.1(c) compare the aftershock fragility for the Complete limit state under Slight, Moderate, and Extensive mainshock damage, respectively. As shown in Figure 5.1(a), if Slight damage occurs under the mainshock, the effect on aftershock vulnerability for the Complete limit state is negligible for the Era 33 and Era 22 bridges. In contrast, if Era 11 bridge incurs Slight damage following the mainshock, the median spectral capacity for the Complete limit state is reduced by about 7% compared to when the bridge is intact following the mainshock. If the damage caused by the mainshock is Moderate or Extensive, the increase in vulnerability is measurable for all three Eras. For the Moderate damage state, (Figure 5.1b), the median spectral intensity corresponding to Complete damage is reduced by 17%, 9% and 5% compared to the Intact state (the bridge remains undamaged when subjected to mainshock), for Eras 11, 22, and 33, respectively. For Extensive mainshock damage, the reduction relative to the Intact state is 23%, 11%, and 7% for Eras 11, 22, and 33, respectively.

Table 5.1 shows the median and dispersion values for the aftershock fragility curves corresponding to the four damage states when the bridge is in the Intact, Slight, Moderate, or Extensive damage states immediately following the mainshock.

Table 5.1 Median (μ) and Dispersion (β) for mainshock and aftershock limit state fragility functions.

Design eras	Damage states	Main shock fragility parameters		Aftershock fragility parameters (no damage under mainshock)		Aftershock fragility parameters (slight damage under mainshock)		Aftershock fragility parameters (moderate damage under mainshock)		Aftershock fragility parameters (extensive damage under mainshock)	
		μ	β	μ	β	μ	β	μ	β	μ	β
Era 11	Slight	0.093	0.588	0.095	0.510	NA	NA	NA	NA	NA	NA
	Moderate	0.238	0.513	0.241	0.504	0.208	0.503	NA	NA	NA	NA
	Extensive	0.609	0.422	0.617	0.431	0.554	0.446	0.522	0.446	NA	NA
	Complete	0.870	0.343	0.873	0.347	0.807	0.390	0.727	0.388	0.674	0.334
Era 22	Slight	0.117	0.479	0.117	0.479	NA	NA	NA	NA	NA	NA
	Moderate	0.562	0.384	0.562	0.384	0.540	0.450	NA	NA	NA	NA
	Extensive	0.804	0.355	0.804	0.355	0.788	0.393	0.772	0.350	NA	NA
	Complete	1.004	0.335	1.004	0.335	0.983	0.364	0.914	0.323	0.890	0.358
Era 33	Slight	0.118	0.469	0.118	0.469	NA	NA	NA	NA	NA	NA
	Moderate	0.562	0.383	0.562	0.383	0.544	0.418	NA	NA	NA	NA
	Extensive	1.003	0.334	1.003	0.334	0.994	0.320	0.984	0.321	NA	NA
	Complete	1.338	0.308	1.338	0.308	1.323	0.310	1.272	0.2994	1.247	0.377

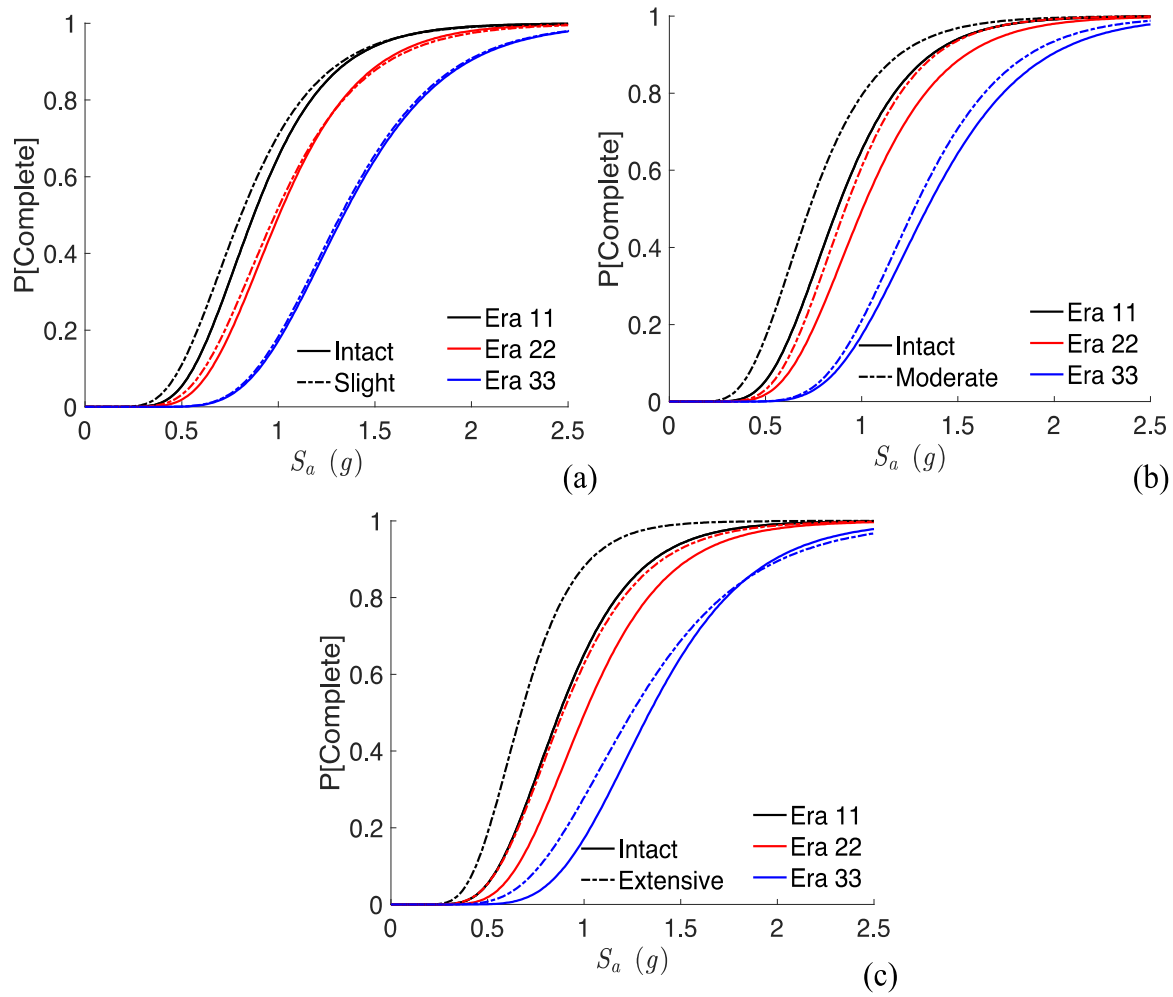


Figure 5.1 Comparing mainshock and aftershock fragility curves corresponding to the (a) Slight, (b) Moderate and (c) Extensive damage states under mainshock.

5.2 Assessing Bridge Aftershock Seismic Risk in the Pre- and Post-Mainshock Environments

This section implements the framework presented in Chapter 3 to assess the seismic risk of the three bridges in the pre- and post-mainshock environment. For the latter, aftershock risk is assessed assuming that the mainshock has occurred, and the damaged state of the bridge is known. A period of 30 days following the mainshock is considered; the likelihood that repairs would occur during this time is not considered. A time increment of 0.001 day is used for the Markov chain analysis since the occurrence of more than one aftershock within such a small duration is highly unlikely. Similar to the underlying assumption used to develop the aftershock hazard curve (Chapter 2), the limit transition probabilities are obtained using Equation (3.5), assuming that the first event in the sequence occurred on the fault that has the highest

contribution to the mainshock seismic hazard; in this case it is the Los Angeles section of the Puente Hills fault.

Figure 5.2 shows the time-dependent aftershock limit state occurrence probabilities obtained when a post-mainshock assessment is performed on the Era 11 bridge. Figures, 5.2(a), 5.2(b), and 5.2(c) are plotted for a different conditioning damage state, i.e., Intact, Slight, and Moderate, respectively. Overall, the limit-state occurrence probabilities decrease—for the conditioning state—and increase sharply—for states more severe than the conditioning state—immediately following the mainshock and converge to a constant value after a few days. The initial rise (or fall) is attributed to a high rate of occurrence of aftershock events in the early days following the mainshock. This observation is explained by the exponential decline in the rate of aftershock events during the days following the mainshock.

Figure 5.2(a) shows that when the Era 11 bridge is in the Intact state following the mainshock, the probability that it remains there drops off (from a value of 1.0) to about 0.5 within days following the event. The probability of Slight or Moderate damage occurring within the same duration is approximately 0.45 (50% of which is attributed to each of the two states), and the probability of more severe damage is negligible. As the severity of the conditioning states increases [e.g., Slight and Moderate as shown in Figure 5.2(b) and Figure 5.2(c), respectively], the likelihood of transitioning to a worst limit state increases. For example, compared to the Intact conditioning state, the likelihood of experiencing the Complete limit state within 30 days of the mainshock increases by 60%, 27%, and 16% in the Era 11, Era 22, and Era 33 bridges when they sustain Moderate damage immediately following the mainshock. The conditional limit-state occurrence probabilities 30 days following the mainshock for all three bridges are summarized in Tables 5.2 to 5.4.

Table 5.2 Conditional limit-state occurrence probabilities for the Era 11 bridge 30 days after the mainshock.

Aftershock Mainshock	Intact	Slight	Moderate	Extensive	Complete
Intact	8.E-01	2.E-01	2.E-02	3.E-04	2.E-05
Slight		1.E+00	3.E-02	5.E-04	5.E-05
Moderate			1.E+00	6.E-04	8.E-05
Extensive				1.E+00	7.E-05
Complete					1.E+00

Table 5.3 Conditional limit-state occurrence probabilities for the Era 22 bridge 30 days after the mainshock.

Aftershock Mainshock	Intact	Slight	Moderate	Extensive	Complete
Intact	9.E-01	1.E-01	3.E-04	3.E-05	6.92E-06
Slight		1.E+00	6.E-04	4.E-05	1.09E-05
Moderate			1.E+00	3.E-05	1.04E-05
Extensive				1.E+00	1.84E-05
Complete					1.E+00

Table 5.4 Conditional limit-state occurrence probabilities for the Era 33 bridge 30 days after the mainshock.

Aftershock Mainshock	Intact	Slight	Moderate	Extensive	Complete
Intact	9.E-01	1.E-01	3.E-04	6.E-06	7.E-07
Slight		1.E+00	5.E-04	5.E-06	8.E-07
Moderate			1.E+00	5.E-06	9.E-07
Extensive				1.E+00	3.E-06
Complete					1.E+00

Next, the seismic risk assessment is carried out in the pre-mainshock environment (i.e., the mainshock–aftershock assessment) using the framework presented in Chapter 3. This type of evaluation accounts for the uncertainty in the occurrence of both mainshocks and aftershocks. Considering a 50-year service life and the aftershock hazard assumed insignificant beyond 30 days after the mainshock, the damage state probability at each time step during the life span of the structure is obtained using an exponential distribution with input rates calculated using Equation (3.7). An underlying assumption in using the exponential distribution to calculate service-life seismic risk is that the bridge is repaired between clusters of mainshock–aftershock events. The low mean annual frequency of exceedance of the limit states (λ_{LS}) summarized in Table 5.5 validates this assumption. More specifically, a low λ_{LS} would allow repairs to be completed, and the bridge returned to the Intact state before potential triggering of a limit-state transition in response to the next cluster of events occurs.

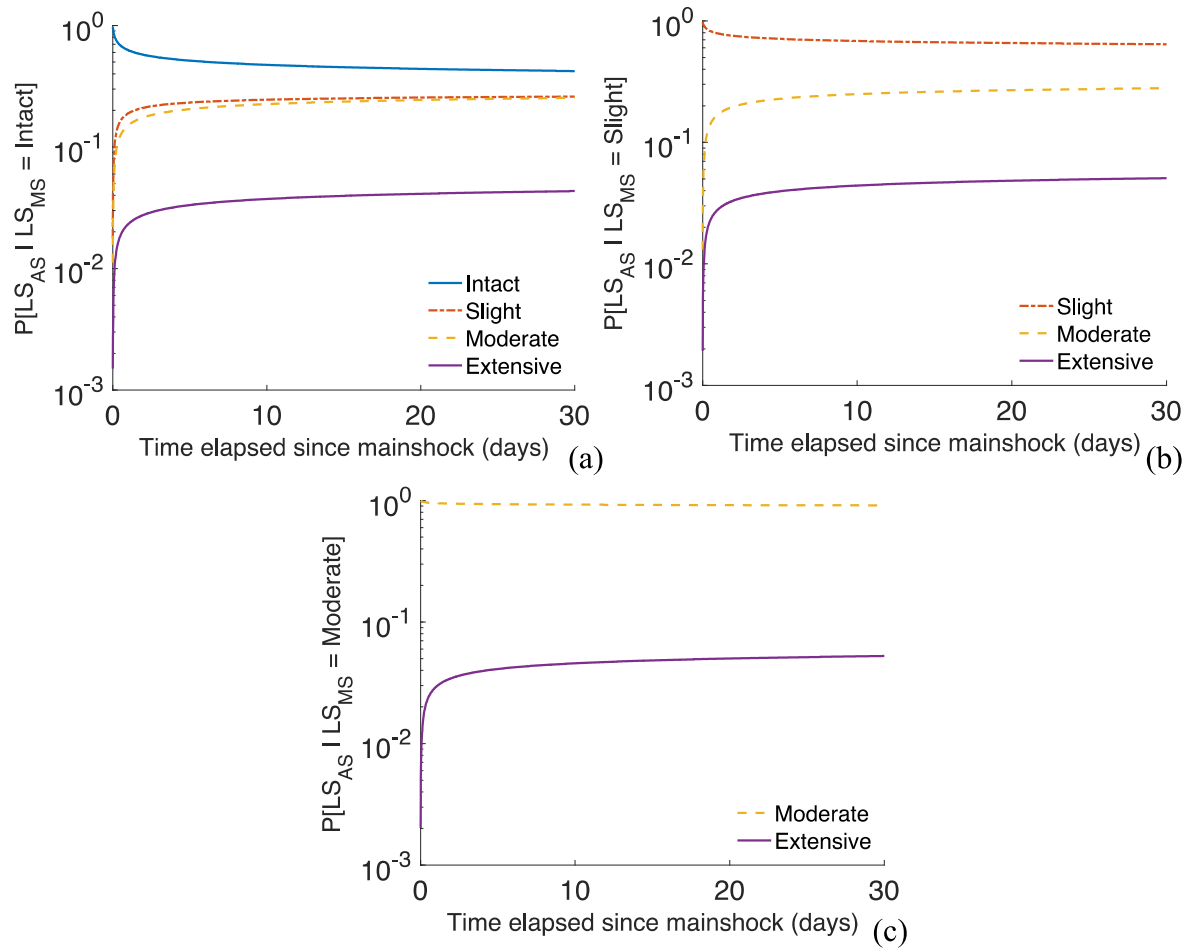


Figure 5.2 Conditional time-dependent limit-state occurrence probabilities in the post-mainshock environment for the Era 11 bridge in the (a) Intact; (b) Slight; and (c) moderate damage states immediately following the mainshock.

Figure 5.3 compares the time-dependent occurrence probabilities for the Slight and Complete limit states for the mainshock-only and mainshock–aftershock assessments. For the former, the effect of aftershocks is not included in the risk analysis. Table 5.6 summarizes the limit state occurrence probabilities at the end of the assumed 50-year service life. The results in Figure 5.3 and Table 5.6 suggest that neglecting the effect of aftershocks leads to a significant underestimation of the service damage for all three bridges. Additionally, the differences between the mainshock-only and mainshock–aftershock assessment results increases with the severity of the limit state and is more significant for the Era 11 bridge, where the 50-year Slight damage probability increases by 25% when aftershocks are considered. For Extensive damage, the 50-year occurrence probability increases by factors of 3.0, 2.5, and 2.0 for the Era 11, Era 22, and Era 33 bridges, respectively.

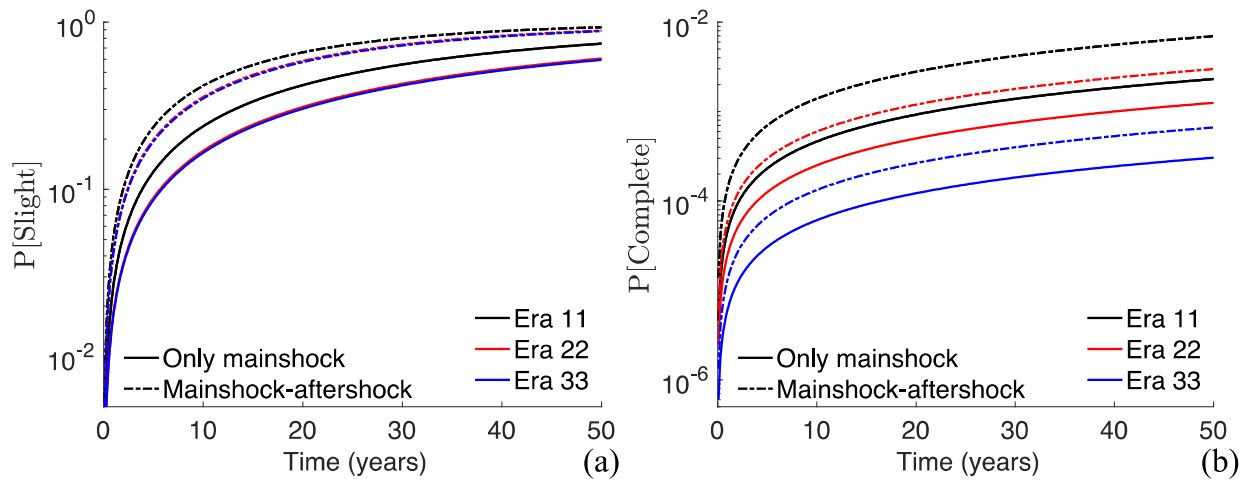


Figure 5.3 Comparing the time-dependent mainshock-only and mainshock-aftershock occurrence probabilities for the (a) Slight and (b) Complete limit states for all three bridges.

Table 5.5 Mean annual frequency of limit-state exceedance in the pre-mainshock environment.

Bridge type	$\lambda_{LS} (\times 10^{-3})$			
	Slight	Moderate	Extensive	Complete
Era 11	53.9	11.9	0.6	0.1
Era 22	44.1	0.6	0.1	0.1
Era 33	43.0	0.6	0.0	0.0

Table 5.6 Limit state occurrence probabilities at the end of the assumed 50-year service life.

Scenario	Bridge	Limit state occurrence probability			
		Slight	Moderate	Extensive	Complete
Mainshock-only	Era 11	0.744	0.191	0.009	0.002
	Era 22	0.606	0.010	0.002	0.001
	Era 33	0.595	0.012	0.001	0.000
Mainshock-aftershock	Era 11	0.932	0.447	0.027	0.007
	Era 22	0.890	0.028	0.005	0.003
	Era 33	0.883	0.031	0.002	0.001

6 Summary and Conclusions

The need for functional bridges increases after a major seismic event because of the role they play in supporting the mobility of first responders. As such, the decision of whether to close a bridge temporarily or permanently after it has been damaged in response to a seismic event is critical. Although this decision is usually influenced by a myriad of factors, ideally the time-dependent risk of further damage caused by aftershocks should be considered.

This study presents a seismic risk assessment for three bridges designed during different eras subjected to the mainshock-only (aftershocks are not considered), aftershock (i.e., conditioned on the known state of the bridge following the mainshock) and mainshock–aftershock (i.e., uncertainty in both the mainshock and aftershock is considered) hazard. The time-dependent nature of aftershock seismic hazard and the uncertainty in the state of the structures in the post-mainshock environment is considered through the use of a Markov-chain framework.

The assessment is performed for three typical California bridges that were built during different design/construction eras: constructed before 1971 (Era 11), constructed between 1971 through 1990 (Era 22), and constructed after 1990 (Era 33). Nonlinear structural models were developed for the three bridges. Based on an assumed location in Southern California, 34 pairs of mainshock and aftershock ground motions were selected for sequential nonlinear RHAs. Seismic vulnerability in the mainshock and aftershock environments was represented using four limit states, denoted as Slight, Moderate, Extensive, and Complete based on the bridge column damage and repair state. Fragility curves were generated initially considering the Intact state and varying level of mainshock damage (as defined by the aforementioned limit states).

For all three design eras, the results from the vulnerability assessment revealed Slight damage under the mainshock had minimum impact on the aftershock performance. For the Era 11 bridge, the effect on aftershock fragility was considerable under more severe forms of mainshock damage (e.g., when the bridge is in the Moderate and Extensive states following the mainshock). The Markov chain-modeling approach was used to perform seismic risk assessments in the pre- and post-mainshock environments. The non-conditioning limit state probabilities for the Era 11 bridge increased sharply within the first few days of the mainshock and plateaued soon after. This observation reflects the high rate of aftershock hazard drop-off

following the mainshock. For the same type of assessment, compared to when the bridge is intact, the probability of Complete damage within 30 days following the mainshock increased by 60%, 27%, and 16% when the Era 11, Era 22, and Era 33 bridges, respectively, are subjected to Moderate mainshock damage.

As noted earlier, the mainshock–aftershock risk assessment considered the uncertainty in the occurrence of both mainshock and aftershocks. Based on an assumed 50-year in-service period and a comparison between the results from the mainshock-only and mainshock–aftershock assessments, the lifetime risk of damage was found to be significantly underestimated if aftershock hazard is ignored. This is especially true for the more severe damage states and older bridges. For instance, the probability of extensive damage within a 50-year period increased by a factor of 3.0 for the Era 11 bridge and 2.0 for the Era 33 bridge. For the Era 11 bridge, accounting for aftershock hazard only increased the 50-year probability of Slight damage by 25%.

Note that the results presented in the current study are for a single bridge configuration (e.g., single column bent and seat abutments) and a hypothetical site. Future studies should consider other bridge configurations (e.g., multi-column bents) and design attributes.

REFERENCES

- Abrahamson N., Silva W.J., Kamai R. (2013). Update of the AS08 ground-motion prediction equations based on the NGA-west2 dataset, *PEER Report No. 2013/04*, Pacific Earthquake Engineering Research Center, University of California, Berkeley, CA.
- Alessandri, S., Giannini R., Paolacci F. (2013). Aftershock risk assessment and the decision to open traffic on bridges, *Earthq. Eng. & Struct. Dyn.*, 42(15): 2255–2275.
- ATC (2017). Guidelines for nonlinear structural analysis for design of buildings, Part IIa, steel moment frames, *ATC-114, NIST-GCR 17-917-46 v2*, National Institute of Standards and Technology, Gaithersburg, MD.
- Baker J.W. (2015). Efficient analytical fragility function fitting using dynamic structural analysis, *Earthq. Spectra*, 31(1): 579–599.
- Baker J.W., Cornell C.A. (2006). Spectral shape, epsilon and record selection, *Earthq. Eng. Struct. Dyn.*, 35(9): 1077–1095.
- Banerjee S., Shinozuka M. (2008). Mechanistic quantification of RC bridge damage states under earthquake through fragility analysis, *Probab. Eng. Mech.*, 23(1): 12–22.
- Bazzurro P., Cornell C.A. (1999). Disaggregation of seismic hazard, *Bull. Seismol. Soc. Am.*, 89(2): 501–520.
- Bommer J.J., Acevedo A.B. (2004). The use of real earthquake accelerograms as input to dynamic analysis, *J. Earthq. Eng.*, 8(01): 43–91.
- Boore D.M., Atkinson G.M. (2008). Ground-motion prediction equations for the average horizontal component of PGA, PGV, and 5%-damped PSA at spectral periods between 0.01 s and 10.0 s. *Earthq. Spectra*, 24: 99–138.
- Boore D.M., Stewart J.P., Seyhan E., Atkinson G.M. (2014). NGA-West2 equations for predicting PGA, PGV, and 5% damped PSA for shallow crustal earthquakes, *Earthq. Spectra*, 30(3): 1057–1085.
- Caltrans (2012). *Personal Communication* with the P266, Task 1780 Fragility project panel members including C. Roblee, M. Yashinsky, M. Mahan, T. Shantz, H. Setberg, L. Turner, S. Sahs, T. Adams, and M. Keever California Department of Transportation. Sacramento. CA.
- Chang G.A., Mander J.B. (1994). Seismic energy based fatigue damage analysis of bridge columns: Part 1: Evaluation of seismic capacity, *Technical Report NCEER-94-0006*, University of Buffalo, State University of New York, Buffalo, NY.
- Chiou B.S.-J., Youngs R.R. (2008). An NGA model for the average horizontal component of peak ground motion and response spectra, *Earthq. Spectra*, 24(1): 173–215.
- Chiou B.S.-J., Darragh R., Gregor N., Silva W.J. (2008). NGA project strong-motion database, *Earthq. Spectra*, 24(1): 23–44.
- FEMA (2012). *HAZUS-MH 2.1: Multi-Hazard Loss Estimation Methodology: Earthquake Model*, Federal Emergency Management Agency, Department of Homeland Security, Washington, D.C.
- Franchin P., Pinto P.E. (2009). Allowing traffic over mainshock-damaged bridges, *J. Earthq. Eng.*, 13(5): 585–599.
- Ghosh J., Padgett J.E., Sánchez-Silva M. (2015). Seismic damage accumulation in highway bridges in earthquake-prone regions, *Earthq. Spectra*, 31(1): 115–135.
- Goda K. (2012). Nonlinear response potential of mainshock–aftershock sequences from Japanese earthquakes, *Bull. Seismol. Soc. Am.*, 102(5): 2139–2156.
- Goda K. (2015). Record selection for aftershock incremental dynamic analysis, *Earthq. Eng. Struct. Dyn.*, 44(7): 1157–1162.
- Haselton C.B., Baker J.W., Liel A.B., Deierlein G.G. (2009). Accounting for ground-motion spectral shape characteristics in structural collapse assessment through an adjustment for epsilon, *Earthq. Eng. Struct. Dyn.*, 137(3): 332–344.

- Hatzigeorgiou G.D., Beskos D.E. (2009). Inelastic displacement ratios for SDOF structures subjected to repeated earthquakes, *Eng. Struct.*, 31(11): 2744–2755.
- Jeon J.S., DesRoches R., Lee D.H. (2016). Post-repair effect of column jackets on aftershock fragilities of damaged RC bridges subjected to successive earthquakes, *Earthq. Eng. Struct. Dyn.*, 45(7): 1149–1168.
- Kalkan E., Chopra A.K. (2010). Practical guidelines to select and scale earthquake records for nonlinear response history analysis of structures, U.S. Geological Survey Open-File Report 2010, U.S. Department of the Interior, Washington, D.C., 113 pgs.
- Knopoff L., Gardner J. (1972). Higher seismic activity during local night on the raw worldwide earthquake catalogue, *Geophys. J. Royal Astro. Soc.*, 28(3): 311–313.
- Kramer S.L. (1996). *Geotechnical Earthquake Engineering*, Prentice Hall: New York.
- Mackie K., Stojadinovic B. (2001). Probabilistic seismic demand model for California highway bridges, *J. Bridge Eng.*, 6(6): 468–481.
- Mackie K., Stojadinović B. (2006). Post-earthquake functionality of highway overpass bridges, *Earthq. Eng. Struct. Dyn.*, 35(1): 77–93.
- Mangalathu S. (2017). *Performance Based Grouping and Fragility Analysis of Box Girder Bridges in California*, Ph.D. Thesis, Department of Civil and Environmental Engineering, Georgia Institute of Technology, Atlanta, GA.
- Mangalathu S., Jeon J.-S. (2018). Adjustment factors to account for the effect of bridge deck horizontal curvature on the seismic response of concrete box-girder bridges in California, *Earthq. Spectra*, 34(2): 893–914.
- Mangalathu S., Jeon J.-S., DesRoches R., Padgett J.E. (2016). ANCOVA-based grouping of bridge classes for seismic fragility assessment, *Eng. Struct.*, 123, 379–394.
- Mangalathu S., Jeon J.-S., DesRoches R. (2018). Critical uncertainty parameters influencing seismic performance of bridges using Lasso regression, *Earthq. Eng. Struct. Dyn.*, 47(3): 784–801.
- Mangalathu S., Soleimani F., Jeon J.-S. (2017). Bridge classes for regional seismic risk assessment: Improving HAZUS models, *Eng. Struct.*, 148: 755–766.
- Megally S.H., Silva F.P., Seible F. (2002). Seismic response of sacrificial shear keys in bridge abutments, Report No. SSRP-2001/23, Final Report to Caltrans Contract No. 59A0051, Department of Structural Engineering, University of California, San Diego, La Jolla, CA.
- Muthukumar S., DesRoches R. (2006). A Hertz contact model with non-linear damping for pounding simulation, *Earthq. Eng. Struct. Dyn.*, 35(7): 811–828.
- Nielson B.G. (2005). *Analytical Fragility Curves for Highway Bridges in Moderate Seismic Zones*, Ph.D. Thesis, Department of Civil and Environmental Engineering, Georgia Institute of Technology, Atlanta, GA.
- Omranian E., Abdelnaby A.E., Abdollahzadeh G. (2018). Seismic vulnerability assessment of RC skew bridges subjected to mainshock-aftershock sequences, *Soil Dyn. Earthq. Eng.*, 114: 186–197.
- Ramanathan K.N. (2012). *Next Generation Seismic Fragility Curves for California Bridges Incorporating the Evolution in Seismic Design Philosophy*, Ph.D. Thesis, Department of Civil and Environmental Engineering, Georgia Institute of Technology, Atlanta, GA.
- Reasenber P.A., Jones L.M. (1989). Earthquake hazard after a mainshock in California, *Science*. 243(4895): 1173–1176.
- Ruiz-García J. (2012). Mainshock-aftershock ground motion features and their influence in building's seismic response, *J. Earthq. Eng.*, 16(5): 719–737.
- Ruiz-García J., Negrete-Manriquez J.C. (2011). Evaluation of drift demands in existing steel frames under as-recorded far-field and near-fault mainshock-aftershock seismic sequences, *Eng. Struct.*, 33(2): 621–634.
- Shamsabadi A., Yan L. (2008). Closed-form force-displacement backbone curves for bridge abutment-backfill systems, American Society of Civil Engineers, *Proceedings, Geotechnical Earthquake Engineering and Soil Dynamics IV Congress*, Sacramento, CA, DOI: 10.1061/40975(318)159.

- Shcherbakov R., Turcotte D.L. (2004). A modified form of Båth's law, *Bull. Seismol. Soc. Am.*, 94(5): 1968–1975.
- Shome N., Cornell C.A., Bazzurro P., Carballo J.E. (1998). Earthquakes, records, and nonlinear responses, *Earthq. Spectra*, 14(3): 469–500.
- Soleimani F., Mangalathu S., DesRoches R. (2017). A comparative analytical study on the fragility assessment of box-girder bridges with various column shapes, *Eng. Struct.*, 153: 460–478.
- Utsu T., Ogata Y., Ritsuko M. (1995). The centenary of the Omori formula for a decay law of aftershock activity, *J. Phys. Earth*, 43(1): 1–33.
- Vosooghi A., Saiidi M.S. (2010). Seismic damage states and response parameters for bridge columns, American Concrete Institute, *Special Publication*, 271: 29–46.
- Wooddell K.E., Abrahamson N.A. (2014). Classification of main shocks and aftershocks in the NGA-West2 database, *Earthq. Spectra*, 30(3): 1257–1267.
- Yeo G.L., Cornell C.A. (2009). A probabilistic framework for quantification of aftershock ground-motion hazard in California: Methodology and parametric study, *Earthq. Eng. Struct. Dyn.*, 38: 45–60.
- Zhang J., Huo Y., Brandenberg S.J., Kashighandi P. (2008). Effects of structural characterizations on fragility functions of bridges subject to seismic shaking and lateral spreading, *Earthq. Eng. Eng. Vib.*, 7(4): 369–382.

PEER REPORTS

PEER reports are available as a free PDF download from <https://peer.berkeley.edu/peer-reports>. In addition, printed hard copies of PEER reports can be ordered directly from our printer by following the instructions at <https://peer.berkeley.edu/peer-reports>. For other related questions about the PEER Report Series, contact the Pacific Earthquake Engineering Research Center, 325 Davis Hall, Mail Code 1792, Berkeley, CA 94720. Tel.: (510) 642-3437; and Email: peer_center@berkeley.edu.

- PEER 2019/03** *Ground-Motion Directivity Modeling for Seismic Hazard Applications*. Jennifer L. Donahue, Jonathan P. Stewart, Nicolas Gregor, and Yousef Bozorgnia. Review Panel: Jonathan D. Bray, Stephen A. Mahin, I. M. Idriss, Robert W. Graves, and Tom Shantz. May 2019.
- PEER 2019/02** *Direct-Finite-Element Method for Nonlinear Earthquake Analysis of Concrete Dams Including Dam–Water–Foundation Rock Interaction*. Arnkjell Løkke and Anil K. Chopra. March 2019.
- PEER 2019/01** *Flow-Failure Case History of the Las Palmas, Chile, Tailings Dam*. R. E. S. Moss, T. R. Gebhart, D. J. Frost, and C. Ledezma. January 2019.
- PEER 2018/08** *Central and Eastern North America Ground-Motion Characterization: NGA-East Final Report*. Christine Goulet, Yousef Bozorgnia, Norman Abrahamson, Nicolas Kuehn, Linda Al Atik, Robert Youngs, Robert Graves, and Gail Atkinson. December 2018.
- PEER 2018/07** *An Empirical Model for Fourier Amplitude Spectra using the NGA-West2 Database*. Jeff Bayless, and Norman A. Abrahamson. December 2018.
- PEER 2018/06** *Estimation of Shear Demands on Rock-Socketed Drilled Shafts subjected to Lateral Loading*. Pedro Arduino, Long Chen, and Christopher R. McGann. December 2018.
- PEER 2018/05** *Selection of Random Vibration Procedures for the NGA-East Project*. Albert Kottke, Norman A. Abrahamson, David M. Boore, Yousef Bozorgnia, Christine Goulet, Justin Hollenback, Tadahiro Kishida, Armen Der Kiureghian, Olga-Joan Ktenidou, Nicolas Kuehn, Ellen M. Rathje, Walter J. Silva, Eric Thompson, and Xiaoyue Wang. December 2018.
- PEER 2018/04** *Capturing Directivity Effects in the Mean and Aleatory Variability of the NGA-West 2 Ground Motion Prediction Equations*. Jennie A. Watson-Lamprey. November 2018.
- PEER 2018/03** *Probabilistic Seismic Hazard Analysis Code Verification*. Christie Hale, Norman Abrahamson, and Yousef Bozorgnia. July 2018.
- PEER 2018/02** *Update of the BCHydro Subduction Ground-Motion Model using the NGA-Subduction Dataset*. Norman Abrahamson, Nicolas Kuehn, Zeynep Gulerce, Nicholas Gregor, Yousef Bozorgnia, Grace Parker, Jonathan Stewart, Brian Chiou, I. M. Idriss, Kenneth Campbell, and Robert Youngs. June 2018.
- PEER 2018/01** *PEER Annual Report 2017–2018*. Khalid Mosalam, Amarnath Kasalanati, and Selim Günay. June 2018.
- PEER 2017/12** *Experimental Investigation of the Behavior of Vintage and Retrofit Concentrically Braced Steel Frames under Cyclic Loading*. Barbara G. Simpson, Stephen A. Mahin, and Jiun-Wei Lai, December 2017.
- PEER 2017/11** *Preliminary Studies on the Dynamic Response of a Seismically Isolated Prototype Gen-IV Sodium-Cooled Fast Reactor (PGSFR)*. Benshun Shao, Andreas H. Schellenberg, Matthew J. Schoettler, and Stephen A. Mahin. December 2017.
- PEER 2017/10** *Development of Time Histories for IEEE693 Testing and Analysis (including Seismically Isolated Equipment)*. Shakhzod M. Takhirov, Eric Fujisaki, Leon Kempner, Michael Riley, and Brian Low. December 2017.
- PEER 2017/09** *“R” Package for Computation of Earthquake Ground-Motion Response Spectra*. Pengfei Wang, Jonathan P. Stewart, Yousef Bozorgnia, David M. Boore, and Tadahiro Kishida. December 2017.
- PEER 2017/08** *Influence of Kinematic SSI on Foundation Input Motions for Bridges on Deep Foundations*. Benjamin J. Turner, Scott J. Brandenburg, and Jonathan P. Stewart. November 2017.
- PEER 2017/07** *A Nonlinear Kinetic Model for Multi-Stage Friction Pendulum Systems*. Paul L. Drazin and Sanjay Govindjee. September 2017.
- PEER 2017/06** *Guidelines for Performance-Based Seismic Design of Tall Buildings, Version 2.02*. TBI Working Group led by co-chairs Ron Hamburger and Jack Moehle: Jack Baker, Jonathan Bray, C.B. Crouse, Greg Deierlein, John Hooper, Marshall Lew, Joe Maffei, Stephen Mahin, James Malley, Farzad Naeim, Jonathan Stewart, and John Wallace. May 2017.
- PEER 2017/05** *Recommendations for Ergodic Nonlinear Site Amplification in Central and Eastern North America*. Youssef M.A. Hashash, Joseph A. Harmon, Okan Ilhan, Grace A. Parker, and Jonathan P. Stewart. March 2017.

- PEER 2017/04** *Expert Panel Recommendations for Ergodic Site Amplification in Central and Eastern North America.* Jonathan P. Stewart, Grace A. Parker, Joseph P. Harmon, Gail M. Atkinson, David M. Boore, Robert B. Darragh, Walter J. Silva, and Youssef M.A. Hashash. March 2017.
- PEER 2017/03** *NGA-East Ground-Motion Models for the U.S. Geological Survey National Seismic Hazard Maps.* Christine A. Goulet, Yousef Bozorgnia, Nicolas Kuehn, Linda Al Atik, Robert R. Youngs, Robert W. Graves, and Gail M. Atkinson. March 2017.
- PEER 2017/02** *U.S.–New Zealand–Japan Workshop: Liquefaction-Induced Ground Movements Effects, University of California, Berkeley, California, 2–4 November 2016.* Jonathan D. Bray, Ross W. Boulanger, Misko Cubrinovski, Kohji Tokimatsu, Steven L. Kramer, Thomas O'Rourke, Ellen Rathje, Russell A. Green, Peter K. Robinson, and Christine Z. Beyzaei. March 2017.
- PEER 2017/01** *2016 PEER Annual Report.* Khalid M. Mosalam, Amarnath Kasalanati, and Grace Kang. March 2017.
- PEER 2016/10** *Performance-Based Robust Nonlinear Seismic Analysis with Application to Reinforced Concrete Bridge Systems.* Xiao Ling and Khalid M. Mosalam. December 2016.
- PEER 2017/09** *Detailing Requirements for Column Plastic Hinges subjected to Combined Flexural, Axial, and Torsional Seismic Loading.* Gabriel Hurtado and Jack P. Moehle. December 2016.
- PEER 2016/08** *Resilience of Critical Structures, Infrastructure, and Communities.* Gian Paolo Cimellaro, Ali Zamani-Noori, Omar Kamouh, Vesna Terzic, and Stephen A. Mahin. December 2016.
- PEER 2016/07** *Hybrid Simulation Theory for a Classical Nonlinear Dynamical System.* Paul L. Drazin and Sanjay Govindjee. September 2016.
- PEER 2016/06** *California Earthquake Early Warning System Benefit Study.* Laurie A. Johnson, Sharyl Rabinovici, Grace S. Kang, and Stephen A. Mahin. July 2006.
- PEER 2016/05** *Ground-Motion Prediction Equations for Arias Intensity Consistent with the NGA-West2 Ground-Motion Models.* Charlotte Abrahamson, Hao-Jun Michael Shi, and Brian Yang. July 2016.
- PEER 2016/04** *The M_w 6.0 South Napa Earthquake of August 24, 2014: A Wake-Up Call for Renewed Investment in Seismic Resilience Across California.* Prepared for the California Seismic Safety Commission, Laurie A. Johnson and Stephen A. Mahin. May 2016.
- PEER 2016/03** *Simulation Confidence in Tsunami-Driven Overland Flow.* Patrick Lynett. May 2016.
- PEER 2016/02** *Semi-Automated Procedure for Windowing time Series and Computing Fourier Amplitude Spectra for the NGA-West2 Database.* Tadahiro Kishida, Olga-Joan Ktenidou, Robert B. Darragh, and Walter J. Silva. May 2016.
- PEER 2016/01** *A Methodology for the Estimation of Kappa (κ) from Large Datasets: Example Application to Rock Sites in the NGA-East Database and Implications on Design Motions.* Olga-Joan Ktenidou, Norman A. Abrahamson, Robert B. Darragh, and Walter J. Silva. April 2016.
- PEER 2015/13** *Self-Centering Precast Concrete Dual-Steel-Shell Columns for Accelerated Bridge Construction: Seismic Performance, Analysis, and Design.* Gabriele Guerrini, José I. Restrepo, Athanassios Vervelidis, and Milena Massari. December 2015.
- PEER 2015/12** *Shear-Flexure Interaction Modeling for Reinforced Concrete Structural Walls and Columns under Reversed Cyclic Loading.* Kristijan Kolozvari, Kutay Orakcal, and John Wallace. December 2015.
- PEER 2015/11** *Selection and Scaling of Ground Motions for Nonlinear Response History Analysis of Buildings in Performance-Based Earthquake Engineering.* N. Simon Kwong and Anil K. Chopra. December 2015.
- PEER 2015/10** *Structural Behavior of Column-Bent Cap Beam-Box Girder Systems in Reinforced Concrete Bridges Subjected to Gravity and Seismic Loads. Part II: Hybrid Simulation and Post-Test Analysis.* Mohamed A. Moustafa and Khalid M. Mosalam. November 2015.
- PEER 2015/09** *Structural Behavior of Column-Bent Cap Beam-Box Girder Systems in Reinforced Concrete Bridges Subjected to Gravity and Seismic Loads. Part I: Pre-Test Analysis and Quasi-Static Experiments.* Mohamed A. Moustafa and Khalid M. Mosalam. September 2015.
- PEER 2015/08** *NGA-East: Adjustments to Median Ground-Motion Models for Center and Eastern North America.* August 2015.
- PEER 2015/07** *NGA-East: Ground-Motion Standard-Deviation Models for Central and Eastern North America.* Linda Al Atik. June 2015.
- PEER 2015/06** *Adjusting Ground-Motion Intensity Measures to a Reference Site for which $V_{S30} = 3000$ m/sec.* David M. Boore. May 2015.

- PEER 2015/05** *Hybrid Simulation of Seismic Isolation Systems Applied to an APR-1400 Nuclear Power Plant.* Andreas H. Schellenberg, Alireza Sarebanha, Matthew J. Schoettler, Gilberto Mosqueda, Gianmario Benzoni, and Stephen A. Mahin. April 2015.
- PEER 2015/04** *NGA-East: Median Ground-Motion Models for the Central and Eastern North America Region.* April 2015.
- PEER 2015/03** *Single Series Solution for the Rectangular Fiber-Reinforced Elastomeric Isolator Compression Modulus.* James M. Kelly and Niel C. Van Engelen. March 2015.
- PEER 2015/02** *A Full-Scale, Single-Column Bridge Bent Tested by Shake-Table Excitation.* Matthew J. Schoettler, José I. Restrepo, Gabriele Guerrini, David E. Duck, and Francesco Carrea. March 2015.
- PEER 2015/01** *Concrete Column Blind Prediction Contest 2010: Outcomes and Observations.* Vesna Terzic, Matthew J. Schoettler, José I. Restrepo, and Stephen A. Mahin. March 2015.
- PEER 2014/20** *Stochastic Modeling and Simulation of Near-Fault Ground Motions for Performance-Based Earthquake Engineering.* Mayssa Dabaghi and Armen Der Kiureghian. December 2014.
- PEER 2014/19** *Seismic Response of a Hybrid Fiber-Reinforced Concrete Bridge Column Detailed for Accelerated Bridge Construction.* Wilson Nguyen, William Trono, Marios Panagiotou, and Claudia P. Ostertag. December 2014.
- PEER 2014/18** *Three-Dimensional Beam-Truss Model for Reinforced Concrete Walls and Slabs Subjected to Cyclic Static or Dynamic Loading.* Yuan Lu, Marios Panagiotou, and Ioannis Koutromanos. December 2014.
- PEER 2014/17** *PEER NGA-East Database.* Christine A. Goulet, Tadahiro Kishida, Timothy D. Ancheta, Chris H. Cramer, Robert B. Darragh, Walter J. Silva, Youssef M.A. Hashash, Joseph Harmon, Jonathan P. Stewart, Katie E. Wooddell, and Robert R. Youngs. October 2014.
- PEER 2014/16** *Guidelines for Performing Hazard-Consistent One-Dimensional Ground Response Analysis for Ground Motion Prediction.* Jonathan P. Stewart, Kioumars Afshari, and Youssef M.A. Hashash. October 2014.
- PEER 2014/15** *NGA-East Regionalization Report: Comparison of Four Crustal Regions within Central and Eastern North America using Waveform Modeling and 5%-Damped Pseudo-Spectral Acceleration Response.* Jennifer Dreiling, Marius P. Isken, Walter D. Mooney, Martin C. Chapman, and Richard W. Godbee. October 2014.
- PEER 2014/14** *Scaling Relations between Seismic Moment and Rupture Area of Earthquakes in Stable Continental Regions.* Paul Somerville. August 2014.
- PEER 2014/13** *PEER Preliminary Notes and Observations on the August 24, 2014, South Napa Earthquake.* Grace S. Kang and Stephen A. Mahin, Editors. September 2014.
- PEER 2014/12** *Reference-Rock Site Conditions for Central and Eastern North America: Part II – Attenuation (Kappa) Definition.* Kenneth W. Campbell, Youssef M.A. Hashash, Byungmin Kim, Albert R. Kottke, Ellen M. Rathje, Walter J. Silva, and Jonathan P. Stewart. August 2014.
- PEER 2014/11** *Reference-Rock Site Conditions for Central and Eastern North America: Part I - Velocity Definition.* Youssef M.A. Hashash, Albert R. Kottke, Jonathan P. Stewart, Kenneth W. Campbell, Byungmin Kim, Ellen M. Rathje, Walter J. Silva, Sissy Nikolaou, and Cheryl Moss. August 2014.
- PEER 2014/10** *Evaluation of Collapse and Non-Collapse of Parallel Bridges Affected by Liquefaction and Lateral Spreading.* Benjamin Turner, Scott J. Brandenberg, and Jonathan P. Stewart. August 2014.
- PEER 2014/09** *PEER Arizona Strong-Motion Database and GMPEs Evaluation.* Tadahiro Kishida, Robert E. Kayen, Olga-Joan Ktenidou, Walter J. Silva, Robert B. Darragh, and Jennie Watson-Lamprey. June 2014.
- PEER 2014/08** *Unbonded Pretensioned Bridge Columns with Rocking Detail.* Jeffrey A. Schaefer, Bryan Kennedy, Marc O. Eberhard, and John F. Stanton. June 2014.
- PEER 2014/07** *Northridge 20 Symposium Summary Report: Impacts, Outcomes, and Next Steps.* May 2014.
- PEER 2014/06** *Report of the Tenth Planning Meeting of NEES/E-Defense Collaborative Research on Earthquake Engineering.* December 2013.
- PEER 2014/05** *Seismic Velocity Site Characterization of Thirty-One Chilean Seismometer Stations by Spectral Analysis of Surface Wave Dispersion.* Robert Kayen, Brad D. Carkin, Skye Corbet, Camilo Pinilla, Allan Ng, Edward Gorbis, and Christine Truong. April 2014.
- PEER 2014/04** *Effect of Vertical Acceleration on Shear Strength of Reinforced Concrete Columns.* Hyerin Lee and Khalid M. Mosalam. April 2014.
- PEER 2014/03** *Retest of Thirty-Year-Old Neoprene Isolation Bearings.* James M. Kelly and Niel C. Van Engelen. March 2014.
- PEER 2014/02** *Theoretical Development of Hybrid Simulation Applied to Plate Structures.* Ahmed A. Bakhty, Khalid M. Mosalam, and Sanjay Govindjee. January 2014.

- PEER 2014/01** *Performance-Based Seismic Assessment of Skewed Bridges*. Peyman Kaviani, Farzin Zareian, and Ertugrul Taciroglu. January 2014.
- PEER 2013/26** *Urban Earthquake Engineering*. Proceedings of the U.S.-Iran Seismic Workshop. December 2013.
- PEER 2013/25** *Earthquake Engineering for Resilient Communities: 2013 PEER Internship Program Research Report Collection*. Heidi Tremayne (Editor), Stephen A. Mahin (Editor), Jorge Archbold Monterossa, Matt Brosman, Shelly Dean, Katherine deLaveaga, Curtis Fong, Donovan Holder, Rakeeb Khan, Elizabeth Jachens, David Lam, Daniela Martinez Lopez, Mara Minner, Geffen Oren, Julia Pavicic, Melissa Quinonez, Lorena Rodriguez, Sean Salazar, Kelli Slaven, Vivian Steyert, Jenny Taing, and Salvador Tena. December 2013.
- PEER 2013/24** *NGA-West2 Ground Motion Prediction Equations for Vertical Ground Motions*. September 2013.
- PEER 2013/23** *Coordinated Planning and Preparedness for Fire Following Major Earthquakes*. Charles Scawthorn. November 2013.
- PEER 2013/22** *GEM-PEER Task 3 Project: Selection of a Global Set of Ground Motion Prediction Equations*. Jonathan P. Stewart, John Douglas, Mohammad B. Javanbarg, Carola Di Alessandro, Yousef Bozorgnia, Norman A. Abrahamson, David M. Boore, Kenneth W. Campbell, Elise Delavaud, Mustafa Erdik, and Peter J. Stafford. December 2013.
- PEER 2013/21** *Seismic Design and Performance of Bridges with Columns on Rocking Foundations*. Grigorios Antonellis and Marios Panagiotou. September 2013.
- PEER 2013/20** *Experimental and Analytical Studies on the Seismic Behavior of Conventional and Hybrid Braced Frames*. Jiun-Wei Lai and Stephen A. Mahin. September 2013.
- PEER 2013/19** *Toward Resilient Communities: A Performance-Based Engineering Framework for Design and Evaluation of the Built Environment*. Michael William Mieler, Bozidar Stojadinovic, Robert J. Budnitz, Stephen A. Mahin, and Mary C. Comerio. September 2013.
- PEER 2013/18** *Identification of Site Parameters that Improve Predictions of Site Amplification*. Ellen M. Rathje and Sara Navidi. July 2013.
- PEER 2013/17** *Response Spectrum Analysis of Concrete Gravity Dams Including Dam-Water-Foundation Interaction*. Arnkjell Løkke and Anil K. Chopra. July 2013.
- PEER 2013/16** *Effect of Hoop Reinforcement Spacing on the Cyclic Response of Large Reinforced Concrete Special Moment Frame Beams*. Marios Panagiotou, Tea Visnjic, Grigorios Antonellis, Panagiotis Galanis, and Jack P. Moehle. June 2013.
- PEER 2013/15** *A Probabilistic Framework to Include the Effects of Near-Fault Directivity in Seismic Hazard Assessment*. Shrey Kumar Shahi, Jack W. Baker. October 2013.
- PEER 2013/14** *Hanging-Wall Scaling using Finite-Fault Simulations*. Jennifer L. Donahue and Norman A. Abrahamson. September 2013.
- PEER 2013/13** *Semi-Empirical Nonlinear Site Amplification and its Application in NEHRP Site Factors*. Jonathan P. Stewart and Emel Seyhan. November 2013.
- PEER 2013/12** *Nonlinear Horizontal Site Response for the NGA-West2 Project*. Ronnie Kamai, Norman A. Abramson, Walter J. Silva. May 2013.
- PEER 2013/11** *Epistemic Uncertainty for NGA-West2 Models*. Linda Al Atik and Robert R. Youngs. May 2013.
- PEER 2013/10** *NGA-West 2 Models for Ground-Motion Directionality*. Shrey K. Shahi and Jack W. Baker. May 2013.
- PEER 2013/09** *Final Report of the NGA-West2 Directivity Working Group*. Paul Spudich, Jeffrey R. Bayless, Jack W. Baker, Brian S.J. Chiou, Badie Rowshandel, Shrey Shahi, and Paul Somerville. May 2013.
- PEER 2013/08** *NGA-West2 Model for Estimating Average Horizontal Values of Pseudo-Absolute Spectral Accelerations Generated by Crustal Earthquakes*. I. M. Idriss. May 2013.
- PEER 2013/07** *Update of the Chiou and Youngs NGA Ground Motion Model for Average Horizontal Component of Peak Ground Motion and Response Spectra*. Brian Chiou and Robert Youngs. May 2013.
- PEER 2013/06** *NGA-West2 Campbell-Bozorgnia Ground Motion Model for the Horizontal Components of PGA, PGV, and 5%-Damped Elastic Pseudo-Acceleration Response Spectra for Periods Ranging from 0.01 to 10 sec*. Kenneth W. Campbell and Yousef Bozorgnia. May 2013.
- PEER 2013/05** *NGA-West 2 Equations for Predicting Response Spectral Accelerations for Shallow Crustal Earthquakes*. David M. Boore, Jonathan P. Stewart, Emel Seyhan, and Gail M. Atkinson. May 2013.

- PEER 2013/04** *Update of the AS08 Ground-Motion Prediction Equations Based on the NGA-West2 Data Set.* Norman Abrahamson, Walter Silva, and Ronnie Kamai. May 2013.
- PEER 2013/03** *PEER NGA-West2 Database.* Timothy D. Ancheta, Robert B. Darragh, Jonathan P. Stewart, Emel Seyhan, Walter J. Silva, Brian S.J. Chiou, Katie E. Wooddell, Robert W. Graves, Albert R. Kottke, David M. Boore, Tadahiro Kishida, and Jennifer L. Donahue. May 2013.
- PEER 2013/02** *Hybrid Simulation of the Seismic Response of Squat Reinforced Concrete Shear Walls.* Catherine A. Whyte and Bozidar Stojadinovic. May 2013.
- PEER 2013/01** *Housing Recovery in Chile: A Qualitative Mid-program Review.* Mary C. Comerio. February 2013.
- PEER 2012/08** *Guidelines for Estimation of Shear Wave Velocity.* Bernard R. Wair, Jason T. DeJong, and Thomas Shantz. December 2012.
- PEER 2012/07** *Earthquake Engineering for Resilient Communities: 2012 PEER Internship Program Research Report Collection.* Heidi Tremayne (Editor), Stephen A. Mahin (Editor), Collin Anderson, Dustin Cook, Michael Erceg, Carlos Esparza, Jose Jimenez, Dorian Krausz, Andrew Lo, Stephanie Lopez, Nicole McCurdy, Paul Shipman, Alexander Strum, Eduardo Vega. December 2012.
- PEER 2012/06** *Fragilities for Precarious Rocks at Yucca Mountain.* Matthew D. Purvance, Rasool Anooshehpour, and James N. Brune. December 2012.
- PEER 2012/05** *Development of Simplified Analysis Procedure for Piles in Laterally Spreading Layered Soils.* Christopher R. McGann, Pedro Arduino, and Peter Mackenzie-Helnwein. December 2012.
- PEER 2012/04** *Unbonded Pre-Tensioned Columns for Bridges in Seismic Regions.* Phillip M. Davis, Todd M. Janes, Marc O. Eberhard, and John F. Stanton. December 2012.
- PEER 2012/03** *Experimental and Analytical Studies on Reinforced Concrete Buildings with Seismically Vulnerable Beam-Column Joints.* Sangjoon Park and Khalid M. Mosalam. October 2012.
- PEER 2012/02** *Seismic Performance of Reinforced Concrete Bridges Allowed to Uplift during Multi-Directional Excitation.* Andres Oscar Espinoza and Stephen A. Mahin. July 2012.
- PEER 2012/01** *Spectral Damping Scaling Factors for Shallow Crustal Earthquakes in Active Tectonic Regions.* Sanaz Rezaeian, Yousef Bozorgnia, I. M. Idriss, Kenneth Campbell, Norman Abrahamson, and Walter Silva. July 2012.
- PEER 2011/10** *Earthquake Engineering for Resilient Communities: 2011 PEER Internship Program Research Report Collection.* Heidi Faison and Stephen A. Mahin, Editors. December 2011.
- PEER 2011/09** *Calibration of Semi-Stochastic Procedure for Simulating High-Frequency Ground Motions.* Jonathan P. Stewart, Emel Seyhan, and Robert W. Graves. December 2011.
- PEER 2011/08** *Water Supply in regard to Fire Following Earthquake.* Charles Scawthorn. November 2011.
- PEER 2011/07** *Seismic Risk Management in Urban Areas.* Proceedings of a U.S.-Iran-Turkey Seismic Workshop. September 2011.
- PEER 2011/06** *The Use of Base Isolation Systems to Achieve Complex Seismic Performance Objectives.* Troy A. Morgan and Stephen A. Mahin. July 2011.
- PEER 2011/05** *Case Studies of the Seismic Performance of Tall Buildings Designed by Alternative Means.* Task 12 Report for the Tall Buildings Initiative. Jack Moehle, Yousef Bozorgnia, Nirmal Jayaram, Pierson Jones, Mohsen Rahnama, Nilesh Shome, Zeynep Tuna, John Wallace, Tony Yang, and Farzin Zareian. July 2011.
- PEER 2011/04** *Recommended Design Practice for Pile Foundations in Laterally Spreading Ground.* Scott A. Ashford, Ross W. Boulanger, and Scott J. Brandenburg. June 2011.
- PEER 2011/03** *New Ground Motion Selection Procedures and Selected Motions for the PEER Transportation Research Program.* Jack W. Baker, Ting Lin, Shrey K. Shahi, and Nirmal Jayaram. March 2011.
- PEER 2011/02** *A Bayesian Network Methodology for Infrastructure Seismic Risk Assessment and Decision Support.* Michelle T. Bensi, Armen Der Kiureghian, and Daniel Straub. March 2011.
- PEER 2011/01** *Demand Fragility Surfaces for Bridges in Liquefied and Laterally Spreading Ground.* Scott J. Brandenburg, Jian Zhang, Pirooz Kashighandi, Yili Huo, and Minxing Zhao. March 2011.
- PEER 2010/05** *Guidelines for Performance-Based Seismic Design of Tall Buildings.* Developed by the Tall Buildings Initiative. November 2010.
- PEER 2010/04** *Application Guide for the Design of Flexible and Rigid Bus Connections between Substation Equipment Subjected to Earthquakes.* Jean-Bernard Dastous and Armen Der Kiureghian. September 2010.

- PEER 2010/03** *Shear Wave Velocity as a Statistical Function of Standard Penetration Test Resistance and Vertical Effective Stress at Caltrans Bridge Sites.* Scott J. Brandenberg, Naresh Bellana, and Thomas Shantz. June 2010.
- PEER 2010/02** *Stochastic Modeling and Simulation of Ground Motions for Performance-Based Earthquake Engineering.* Sanaz Rezaeian and Armen Der Kiureghian. June 2010.
- PEER 2010/01** *Structural Response and Cost Characterization of Bridge Construction Using Seismic Performance Enhancement Strategies.* Ady Aviram, Božidar Stojadinović, Gustavo J. Parra-Montesinos, and Kevin R. Mackie. March 2010.
- PEER 2009/03** *The Integration of Experimental and Simulation Data in the Study of Reinforced Concrete Bridge Systems Including Soil-Foundation-Structure Interaction.* Matthew Dryden and Gregory L. Fenves. November 2009.
- PEER 2009/02** *Improving Earthquake Mitigation through Innovations and Applications in Seismic Science, Engineering, Communication, and Response.* Proceedings of a U.S.-Iran Seismic Workshop. October 2009.
- PEER 2009/01** *Evaluation of Ground Motion Selection and Modification Methods: Predicting Median Interstory Drift Response of Buildings.* Curt B. Haselton, Editor. June 2009.
- PEER 2008/10** *Technical Manual for Strata.* Albert R. Kottke and Ellen M. Rathje. February 2009.
- PEER 2008/09** *NGA Model for Average Horizontal Component of Peak Ground Motion and Response Spectra.* Brian S.-J. Chiou and Robert R. Youngs. November 2008.
- PEER 2008/08** *Toward Earthquake-Resistant Design of Concentrically Braced Steel Structures.* Patxi Uriz and Stephen A. Mahin. November 2008.
- PEER 2008/07** *Using OpenSees for Performance-Based Evaluation of Bridges on Liquefiable Soils.* Stephen L. Kramer, Pedro Arduino, and HyungSuk Shin. November 2008.
- PEER 2008/06** *Shaking Table Tests and Numerical Investigation of Self-Centering Reinforced Concrete Bridge Columns.* Hyung IL Jeong, Junichi Sakai, and Stephen A. Mahin. September 2008.
- PEER 2008/05** *Performance-Based Earthquake Engineering Design Evaluation Procedure for Bridge Foundations Undergoing Liquefaction-Induced Lateral Ground Displacement.* Christian A. Ledezma and Jonathan D. Bray. August 2008.
- PEER 2008/04** *Benchmarking of Nonlinear Geotechnical Ground Response Analysis Procedures.* Jonathan P. Stewart, Annie On-Lei Kwok, Youssef M. A. Hashash, Neven Matasovic, Robert Pyke, Zhiliang Wang, and Zhaohui Yang. August 2008.
- PEER 2008/03** *Guidelines for Nonlinear Analysis of Bridge Structures in California.* Ady Aviram, Kevin R. Mackie, and Božidar Stojadinović. August 2008.
- PEER 2008/02** *Treatment of Uncertainties in Seismic-Risk Analysis of Transportation Systems.* Evangelos Stergiou and Anne S. Kiremidjian. July 2008.
- PEER 2008/01** *Seismic Performance Objectives for Tall Buildings.* William T. Holmes, Charles Kircher, William Petak, and Nabih Youssef. August 2008.
- PEER 2007/12** *An Assessment to Benchmark the Seismic Performance of a Code-Conforming Reinforced Concrete Moment-Frame Building.* Curt Haselton, Christine A. Goulet, Judith Mitrani-Reiser, James L. Beck, Gregory G. Deierlein, Keith A. Porter, Jonathan P. Stewart, and Ertugrul Taciroglu. August 2008.
- PEER 2007/11** *Bar Buckling in Reinforced Concrete Bridge Columns.* Wayne A. Brown, Dawn E. Lehman, and John F. Stanton. February 2008.
- PEER 2007/10** *Computational Modeling of Progressive Collapse in Reinforced Concrete Frame Structures.* Mohamed M. Talaat and Khalid M. Mosalam. May 2008.
- PEER 2007/09** *Integrated Probabilistic Performance-Based Evaluation of Benchmark Reinforced Concrete Bridges.* Kevin R. Mackie, John-Michael Wong, and Božidar Stojadinović. January 2008.
- PEER 2007/08** *Assessing Seismic Collapse Safety of Modern Reinforced Concrete Moment-Frame Buildings.* Curt B. Haselton and Gregory G. Deierlein. February 2008.
- PEER 2007/07** *Performance Modeling Strategies for Modern Reinforced Concrete Bridge Columns.* Michael P. Berry and Marc O. Eberhard. April 2008.
- PEER 2007/06** *Development of Improved Procedures for Seismic Design of Buried and Partially Buried Structures.* Linda Al Atik and Nicholas Sitar. June 2007.
- PEER 2007/05** *Uncertainty and Correlation in Seismic Risk Assessment of Transportation Systems.* Renee G. Lee and Anne S. Kiremidjian. July 2007.

- PEER 2007/04** *Numerical Models for Analysis and Performance-Based Design of Shallow Foundations Subjected to Seismic Loading.* Sivapalan Gajan, Tara C. Hutchinson, Bruce L. Kutter, Prishati Raychowdhury, José A. Ugalde, and Jonathan P. Stewart. May 2008.
- PEER 2007/03** *Beam-Column Element Model Calibrated for Predicting Flexural Response Leading to Global Collapse of RC Frame Buildings.* Curt B. Haselton, Abbie B. Liel, Sarah Taylor Lange, and Gregory G. Deierlein. May 2008.
- PEER 2007/02** *Campbell-Bozorgnia NGA Ground Motion Relations for the Geometric Mean Horizontal Component of Peak and Spectral Ground Motion Parameters.* Kenneth W. Campbell and Yousef Bozorgnia. May 2007.
- PEER 2007/01** *Boore-Atkinson NGA Ground Motion Relations for the Geometric Mean Horizontal Component of Peak and Spectral Ground Motion Parameters.* David M. Boore and Gail M. Atkinson. May 2007.
- PEER 2006/12** *Societal Implications of Performance-Based Earthquake Engineering.* Peter J. May. May 2007.
- PEER 2006/11** *Probabilistic Seismic Demand Analysis Using Advanced Ground Motion Intensity Measures, Attenuation Relationships, and Near-Fault Effects.* Polsak Tothong and C. Allin Cornell. March 2007.
- PEER 2006/10** *Application of the PEER PBEE Methodology to the I-880 Viaduct.* Sashi Kunnath. February 2007.
- PEER 2006/09** *Quantifying Economic Losses from Travel Forgone Following a Large Metropolitan Earthquake.* James Moore, Sungbin Cho, Yue Yue Fan, and Stuart Werner. November 2006.
- PEER 2006/08** *Vector-Valued Ground Motion Intensity Measures for Probabilistic Seismic Demand Analysis.* Jack W. Baker and C. Allin Cornell. October 2006.
- PEER 2006/07** *Analytical Modeling of Reinforced Concrete Walls for Predicting Flexural and Coupled-Shear-Flexural Responses.* Kutay Orakcal, Leonardo M. Massone, and John W. Wallace. October 2006.
- PEER 2006/06** *Nonlinear Analysis of a Soil-Drilled Pier System under Static and Dynamic Axial Loading.* Gang Wang and Nicholas Sitar. November 2006.
- PEER 2006/05** *Advanced Seismic Assessment Guidelines.* Paolo Bazzurro, C. Allin Cornell, Charles Menun, Maziar Motahari, and Nicolas Luco. September 2006.
- PEER 2006/04** *Probabilistic Seismic Evaluation of Reinforced Concrete Structural Components and Systems.* Tae Hyung Lee and Khalid M. Mosalam. August 2006.
- PEER 2006/03** *Performance of Lifelines Subjected to Lateral Spreading.* Scott A. Ashford and Teerawat Juirnarongrit. July 2006.
- PEER 2006/02** *Pacific Earthquake Engineering Research Center Highway Demonstration Project.* Anne Kiremidjian, James Moore, Yue Yue Fan, Nesrin Basoz, Ozgur Yazali, and Meredith Williams. April 2006.
- PEER 2006/01** *Bracing Berkeley. A Guide to Seismic Safety on the UC Berkeley Campus.* Mary C. Comerio, Stephen Tobriner, and Ariane Fehrenkamp. January 2006.
- PEER 2005/17** *Earthquake Simulation Tests on Reducing Residual Displacements of Reinforced Concrete Bridges.* Junichi Sakai, Stephen A Mahin, and Andres Espinoza. December 2005.
- PEER 2005/16** *Seismic Response and Reliability of Electrical Substation Equipment and Systems.* Junho Song, Armen Der Kiureghian, and Jerome L. Sackman. April 2006.
- PEER 2005/15** *CPT-Based Probabilistic Assessment of Seismic Soil Liquefaction Initiation.* R. E. S. Moss, R. B. Seed, R. E. Kayen, J. P. Stewart, and A. Der Kiureghian. April 2006.
- PEER 2005/14** *Workshop on Modeling of Nonlinear Cyclic Load-Deformation Behavior of Shallow Foundations.* Bruce L. Kutter, Geoffrey Martin, Tara Hutchinson, Chad Harden, Sivapalan Gajan, and Justin Phalen. March 2006.
- PEER 2005/13** *Stochastic Characterization and Decision Bases under Time-Dependent Aftershock Risk in Performance-Based Earthquake Engineering.* Gee Liek Yeo and C. Allin Cornell. July 2005.
- PEER 2005/12** *PEER Testbed Study on a Laboratory Building: Exercising Seismic Performance Assessment.* Mary C. Comerio, Editor. November 2005.
- PEER 2005/11** *Van Nuys Hotel Building Testbed Report: Exercising Seismic Performance Assessment.* Helmut Krawinkler, Editor. October 2005.
- PEER 2005/10** *First NEES/E-Defense Workshop on Collapse Simulation of Reinforced Concrete Building Structures.* September 2005.
- PEER 2005/09** *Test Applications of Advanced Seismic Assessment Guidelines.* Joe Maffei, Karl Telleen, Danya Mohr, William Holmes, and Yuki Nakayama. August 2006.

- PEER 2005/08** *Damage Accumulation in Lightly Confined Reinforced Concrete Bridge Columns.* R. Tyler Ranf, Jared M. Nelson, Zach Price, Marc O. Eberhard, and John F. Stanton. April 2006.
- PEER 2005/07** *Experimental and Analytical Studies on the Seismic Response of Freestanding and Anchored Laboratory Equipment.* Dimitrios Konstantinidis and Nicos Makris. January 2005.
- PEER 2005/06** *Global Collapse of Frame Structures under Seismic Excitations.* Luis F. Ibarra and Helmut Krawinkler. September 2005.
- PEER 2005/05** *Performance Characterization of Bench- and Shelf-Mounted Equipment.* Samit Ray Chaudhuri and Tara C. Hutchinson. May 2006.
- PEER 2005/04** *Numerical Modeling of the Nonlinear Cyclic Response of Shallow Foundations.* Chad Harden, Tara Hutchinson, Geoffrey R. Martin, and Bruce L. Kutter. August 2005.
- PEER 2005/03** *A Taxonomy of Building Components for Performance-Based Earthquake Engineering.* Keith A. Porter. September 2005.
- PEER 2005/02** *Fragility Basis for California Highway Overpass Bridge Seismic Decision Making.* Kevin R. Mackie and Božidar Stojadinović. June 2005.
- PEER 2005/01** *Empirical Characterization of Site Conditions on Strong Ground Motion.* Jonathan P. Stewart, Yoojoong Choi, and Robert W. Graves. June 2005.
- PEER 2004/09** *Electrical Substation Equipment Interaction: Experimental Rigid Conductor Studies.* Christopher Stearns and André Filiatrault. February 2005.
- PEER 2004/08** *Seismic Qualification and Fragility Testing of Line Break 550-kV Disconnect Switches.* Shakhzod M. Takhirov, Gregory L. Fenves, and Eric Fujisaki. January 2005.
- PEER 2004/07** *Ground Motions for Earthquake Simulator Qualification of Electrical Substation Equipment.* Shakhzod M. Takhirov, Gregory L. Fenves, Eric Fujisaki, and Don Clyde. January 2005.
- PEER 2004/06** *Performance-Based Regulation and Regulatory Regimes.* Peter J. May and Chris Koski. September 2004.
- PEER 2004/05** *Performance-Based Seismic Design Concepts and Implementation: Proceedings of an International Workshop.* Peter Fajfar and Helmut Krawinkler, Editors. September 2004.
- PEER 2004/04** *Seismic Performance of an Instrumented Tilt-up Wall Building.* James C. Anderson and Vitelmo V. Bertero. July 2004.
- PEER 2004/03** *Evaluation and Application of Concrete Tilt-up Assessment Methodologies.* Timothy Graf and James O. Malley. October 2004.
- PEER 2004/02** *Analytical Investigations of New Methods for Reducing Residual Displacements of Reinforced Concrete Bridge Columns.* Junichi Sakai and Stephen A. Mahin. August 2004.
- PEER 2004/01** *Seismic Performance of Masonry Buildings and Design Implications.* Kerri Anne Taeko Tokoro, James C. Anderson, and Vitelmo V. Bertero. February 2004.
- PEER 2003/18** *Performance Models for Flexural Damage in Reinforced Concrete Columns.* Michael Berry and Marc Eberhard. August 2003.
- PEER 2003/17** *Predicting Earthquake Damage in Older Reinforced Concrete Beam-Column Joints.* Catherine Pagni and Laura Lowes. October 2004.
- PEER 2003/16** *Seismic Demands for Performance-Based Design of Bridges.* Kevin Mackie and Božidar Stojadinović. August 2003.
- PEER 2003/15** *Seismic Demands for Nondeteriorating Frame Structures and Their Dependence on Ground Motions.* Ricardo Antonio Medina and Helmut Krawinkler. May 2004.
- PEER 2003/14** *Finite Element Reliability and Sensitivity Methods for Performance-Based Earthquake Engineering.* Terje Haukaas and Armen Der Kiureghian. April 2004.
- PEER 2003/13** *Effects of Connection Hysteretic Degradation on the Seismic Behavior of Steel Moment-Resisting Frames.* Janise E. Rodgers and Stephen A. Mahin. March 2004.
- PEER 2003/12** *Implementation Manual for the Seismic Protection of Laboratory Contents: Format and Case Studies.* William T. Holmes and Mary C. Comerio. October 2003.
- PEER 2003/11** *Fifth U.S.-Japan Workshop on Performance-Based Earthquake Engineering Methodology for Reinforced Concrete Building Structures.* February 2004.

- PEER 2003/10** *A Beam-Column Joint Model for Simulating the Earthquake Response of Reinforced Concrete Frames.* Laura N. Lowes, Nilanjan Mitra, and Arash Altoontash. February 2004.
- PEER 2003/09** *Sequencing Repairs after an Earthquake: An Economic Approach.* Marco Casari and Simon J. Wilkie. April 2004.
- PEER 2003/08** *A Technical Framework for Probability-Based Demand and Capacity Factor Design (DCFD) Seismic Formats.* Fatemeh Jalayer and C. Allin Cornell. November 2003.
- PEER 2003/07** *Uncertainty Specification and Propagation for Loss Estimation Using FOSM Methods.* Jack W. Baker and C. Allin Cornell. September 2003.
- PEER 2003/06** *Performance of Circular Reinforced Concrete Bridge Columns under Bidirectional Earthquake Loading.* Mahmoud M. Hachem, Stephen A. Mahin, and Jack P. Moehle. February 2003.
- PEER 2003/05** *Response Assessment for Building-Specific Loss Estimation.* Eduardo Miranda and Shahram Taghavi. September 2003.
- PEER 2003/04** *Experimental Assessment of Columns with Short Lap Splices Subjected to Cyclic Loads.* Murat Melek, John W. Wallace, and Joel Conte. April 2003.
- PEER 2003/03** *Probabilistic Response Assessment for Building-Specific Loss Estimation.* Eduardo Miranda and Hesameddin Aslani. September 2003.
- PEER 2003/02** *Software Framework for Collaborative Development of Nonlinear Dynamic Analysis Program.* Jun Peng and Kincho H. Law. September 2003.
- PEER 2003/01** *Shake Table Tests and Analytical Studies on the Gravity Load Collapse of Reinforced Concrete Frames.* Kenneth John Elwood and Jack P. Moehle. November 2003.
- PEER 2002/24** *Performance of Beam to Column Bridge Joints Subjected to a Large Velocity Pulse.* Natalie Gibson, André Filiatrault, and Scott A. Ashford. April 2002.
- PEER 2002/23** *Effects of Large Velocity Pulses on Reinforced Concrete Bridge Columns.* Greg L. Orozco and Scott A. Ashford. April 2002.
- PEER 2002/22** *Characterization of Large Velocity Pulses for Laboratory Testing.* Kenneth E. Cox and Scott A. Ashford. April 2002.
- PEER 2002/21** *Fourth U.S.-Japan Workshop on Performance-Based Earthquake Engineering Methodology for Reinforced Concrete Building Structures.* December 2002.
- PEER 2002/20** *Barriers to Adoption and Implementation of PBEE Innovations.* Peter J. May. August 2002.
- PEER 2002/19** *Economic-Engineered Integrated Models for Earthquakes: Socioeconomic Impacts.* Peter Gordon, James E. Moore II, and Harry W. Richardson. July 2002.
- PEER 2002/18** *Assessment of Reinforced Concrete Building Exterior Joints with Substandard Details.* Chris P. Pantelides, Jon Hansen, Justin Nadauld, and Lawrence D. Reaveley. May 2002.
- PEER 2002/17** *Structural Characterization and Seismic Response Analysis of a Highway Overcrossing Equipped with Elastomeric Bearings and Fluid Dampers: A Case Study.* Nicos Makris and Jian Zhang. November 2002.
- PEER 2002/16** *Estimation of Uncertainty in Geotechnical Properties for Performance-Based Earthquake Engineering.* Allen L. Jones, Steven L. Kramer, and Pedro Arduino. December 2002.
- PEER 2002/15** *Seismic Behavior of Bridge Columns Subjected to Various Loading Patterns.* Asadollah Esmaeily-Gh. and Yan Xiao. December 2002.
- PEER 2002/14** *Inelastic Seismic Response of Extended Pile Shaft Supported Bridge Structures.* T.C. Hutchinson, R.W. Boulanger, Y.H. Chai, and I.M. Idriss. December 2002.
- PEER 2002/13** *Probabilistic Models and Fragility Estimates for Bridge Components and Systems.* Paolo Gardoni, Armen Der Kiureghian, and Khalid M. Mosalam. June 2002.
- PEER 2002/12** *Effects of Fault Dip and Slip Rake on Near-Source Ground Motions: Why Chi-Chi Was a Relatively Mild M7.6 Earthquake.* Brad T. Aagaard, John F. Hall, and Thomas H. Heaton. December 2002.
- PEER 2002/11** *Analytical and Experimental Study of Fiber-Reinforced Strip Isolators.* James M. Kelly and Shakhzod M. Takhirov. September 2002.
- PEER 2002/10** *Centrifuge Modeling of Settlement and Lateral Spreading with Comparisons to Numerical Analyses.* Sivapalan Gajan and Bruce L. Kutter. January 2003.

- PEER 2002/09** *Documentation and Analysis of Field Case Histories of Seismic Compression during the 1994 Northridge, California, Earthquake.* Jonathan P. Stewart, Patrick M. Smith, Daniel H. Whang, and Jonathan D. Bray. October 2002.
- PEER 2002/08** *Component Testing, Stability Analysis and Characterization of Buckling-Restrained Unbonded Braces™.* Cameron Black, Nicos Makris, and Ian Aiken. September 2002.
- PEER 2002/07** *Seismic Performance of Pile-Wharf Connections.* Charles W. Roeder, Robert Graff, Jennifer Soderstrom, and Jun Han Yoo. December 2001.
- PEER 2002/06** *The Use of Benefit-Cost Analysis for Evaluation of Performance-Based Earthquake Engineering Decisions.* Richard O. Zerbe and Anthony Falit-Baiamonte. September 2001.
- PEER 2002/05** *Guidelines, Specifications, and Seismic Performance Characterization of Nonstructural Building Components and Equipment.* André Filiatrault, Constantin Christopoulos, and Christopher Stearns. September 2001.
- PEER 2002/04** *Consortium of Organizations for Strong-Motion Observation Systems and the Pacific Earthquake Engineering Research Center Lifelines Program: Invited Workshop on Archiving and Web Dissemination of Geotechnical Data, 4–5 October 2001.* September 2002.
- PEER 2002/03** *Investigation of Sensitivity of Building Loss Estimates to Major Uncertain Variables for the Van Nuys Testbed.* Keith A. Porter, James L. Beck, and Rustem V. Shaikhutdinov. August 2002.
- PEER 2002/02** *The Third U.S.-Japan Workshop on Performance-Based Earthquake Engineering Methodology for Reinforced Concrete Building Structures.* July 2002.
- PEER 2002/01** *Nonstructural Loss Estimation: The UC Berkeley Case Study.* Mary C. Comerio and John C. Stallmeyer. December 2001.
- PEER 2001/16** *Statistics of SDF-System Estimate of Roof Displacement for Pushover Analysis of Buildings.* Anil K. Chopra, Rakesh K. Goel, and Chatpan Chintanapakdee. December 2001.
- PEER 2001/15** *Damage to Bridges during the 2001 Nisqually Earthquake.* R. Tyler Ranf, Marc O. Eberhard, and Michael P. Berry. November 2001.
- PEER 2001/14** *Rocking Response of Equipment Anchored to a Base Foundation.* Nicos Makris and Cameron J. Black. September 2001.
- PEER 2001/13** *Modeling Soil Liquefaction Hazards for Performance-Based Earthquake Engineering.* Steven L. Kramer and Ahmed-W. Elgamel. February 2001.
- PEER 2001/12** *Development of Geotechnical Capabilities in OpenSees.* Boris Jeremić. September 2001.
- PEER 2001/11** *Analytical and Experimental Study of Fiber-Reinforced Elastomeric Isolators.* James M. Kelly and Shakhzod M. Takhirov. September 2001.
- PEER 2001/10** *Amplification Factors for Spectral Acceleration in Active Regions.* Jonathan P. Stewart, Andrew H. Liu, Yoojoong Choi, and Mehmet B. Baturay. December 2001.
- PEER 2001/09** *Ground Motion Evaluation Procedures for Performance-Based Design.* Jonathan P. Stewart, Shyh-Jeng Chiou, Jonathan D. Bray, Robert W. Graves, Paul G. Somerville, and Norman A. Abrahamson. September 2001.
- PEER 2001/08** *Experimental and Computational Evaluation of Reinforced Concrete Bridge Beam-Column Connections for Seismic Performance.* Clay J. Naito, Jack P. Moehle, and Khalid M. Mosalam. November 2001.
- PEER 2001/07** *The Rocking Spectrum and the Shortcomings of Design Guidelines.* Nicos Makris and Dimitrios Konstantinidis. August 2001.
- PEER 2001/06** *Development of an Electrical Substation Equipment Performance Database for Evaluation of Equipment Fragilities.* Thalia Agnanos. April 1999.
- PEER 2001/05** *Stiffness Analysis of Fiber-Reinforced Elastomeric Isolators.* Hsiang-Chuan Tsai and James M. Kelly. May 2001.
- PEER 2001/04** *Organizational and Societal Considerations for Performance-Based Earthquake Engineering.* Peter J. May. April 2001.
- PEER 2001/03** *A Modal Pushover Analysis Procedure to Estimate Seismic Demands for Buildings: Theory and Preliminary Evaluation.* Anil K. Chopra and Rakesh K. Goel. January 2001.
- PEER 2001/02** *Seismic Response Analysis of Highway Overcrossings Including Soil-Structure Interaction.* Jian Zhang and Nicos Makris. March 2001.
- PEER 2001/01** *Experimental Study of Large Seismic Steel Beam-to-Column Connections.* Egor P. Popov and Shakhzod M. Takhirov. November 2000.

- PEER 2000/10** *The Second U.S.-Japan Workshop on Performance-Based Earthquake Engineering Methodology for Reinforced Concrete Building Structures.* March 2000.
- PEER 2000/09** *Structural Engineering Reconnaissance of the August 17, 1999 Earthquake: Kocaeli (Izmit), Turkey.* Halil Sezen, Kenneth J. Elwood, Andrew S. Whittaker, Khalid Mosalam, John J. Wallace, and John F. Stanton. December 2000.
- PEER 2000/08** *Behavior of Reinforced Concrete Bridge Columns Having Varying Aspect Ratios and Varying Lengths of Confinement.* Anthony J. Calderone, Dawn E. Lehman, and Jack P. Moehle. January 2001.
- PEER 2000/07** *Cover-Plate and Flange-Plate Reinforced Steel Moment-Resisting Connections.* Taejin Kim, Andrew S. Whittaker, Amir S. Gilani, Vitelmo V. Bertero, and Shakhzod M. Takhirov. September 2000.
- PEER 2000/06** *Seismic Evaluation and Analysis of 230-kV Disconnect Switches.* Amir S. J. Gilani, Andrew S. Whittaker, Gregory L. Fenves, Chun-Hao Chen, Henry Ho, and Eric Fujisaki. July 2000.
- PEER 2000/05** *Performance-Based Evaluation of Exterior Reinforced Concrete Building Joints for Seismic Excitation.* Chandra Clyde, Chris P. Pantelides, and Lawrence D. Reaveley. July 2000.
- PEER 2000/04** *An Evaluation of Seismic Energy Demand: An Attenuation Approach.* Chung-Che Chou and Chia-Ming Uang. July 1999.
- PEER 2000/03** *Framing Earthquake Retrofitting Decisions: The Case of Hillside Homes in Los Angeles.* Detlof von Winterfeldt, Nels Roselund, and Alicia Kitsuse. March 2000.
- PEER 2000/02** *U.S.-Japan Workshop on the Effects of Near-Field Earthquake Shaking.* Andrew Whittaker, Editor. July 2000.
- PEER 2000/01** *Further Studies on Seismic Interaction in Interconnected Electrical Substation Equipment.* Armen Der Kiureghian, Kee-Jeung Hong, and Jerome L. Sackman. November 1999.
- PEER 1999/14** *Seismic Evaluation and Retrofit of 230-kV Porcelain Transformer Bushings.* Amir S. Gilani, Andrew S. Whittaker, Gregory L. Fenves, and Eric Fujisaki. December 1999.
- PEER 1999/13** *Building Vulnerability Studies: Modeling and Evaluation of Tilt-up and Steel Reinforced Concrete Buildings.* John W. Wallace, Jonathan P. Stewart, and Andrew S. Whittaker, Editors. December 1999.
- PEER 1999/12** *Rehabilitation of Nonductile RC Frame Building Using Encasement Plates and Energy-Dissipating Devices.* Mehrdad Sasani, Vitelmo V. Bertero, James C. Anderson. December 1999.
- PEER 1999/11** *Performance Evaluation Database for Concrete Bridge Components and Systems under Simulated Seismic Loads.* Yael D. Hose and Frieder Seible. November 1999.
- PEER 1999/10** *U.S.-Japan Workshop on Performance-Based Earthquake Engineering Methodology for Reinforced Concrete Building Structures.* December 1999.
- PEER 1999/09** *Performance Improvement of Long Period Building Structures Subjected to Severe Pulse-Type Ground Motions.* James C. Anderson, Vitelmo V. Bertero, and Raul Bertero. October 1999.
- PEER 1999/08** *Envelopes for Seismic Response Vectors.* Charles Menun and Armen Der Kiureghian. July 1999.
- PEER 1999/07** *Documentation of Strengths and Weaknesses of Current Computer Analysis Methods for Seismic Performance of Reinforced Concrete Members.* William F. Cofer. November 1999.
- PEER 1999/06** *Rocking Response and Overturning of Anchored Equipment under Seismic Excitations.* Nicos Makris and Jian Zhang. November 1999.
- PEER 1999/05** *Seismic Evaluation of 550 kV Porcelain Transformer Bushings.* Amir S. Gilani, Andrew S. Whittaker, Gregory L. Fenves, and Eric Fujisaki. October 1999.
- PEER 1999/04** *Adoption and Enforcement of Earthquake Risk-Reduction Measures.* Peter J. May, Raymond J. Burby, T. Jens Feeley, and Robert Wood. August 1999.
- PEER 1999/03** *Task 3 Characterization of Site Response General Site Categories.* Adrian Rodriguez-Marek, Jonathan D. Bray and Norman Abrahamson. February 1999.
- PEER 1999/02** *Capacity-Demand-Diagram Methods for Estimating Seismic Deformation of Inelastic Structures: SDF Systems.* Anil K. Chopra and Rakesh Goel. April 1999.
- PEER 1999/01** *Interaction in Interconnected Electrical Substation Equipment Subjected to Earthquake Ground Motions.* Armen Der Kiureghian, Jerome L. Sackman, and Kee-Jeung Hong. February 1999.
- PEER 1998/08** *Behavior and Failure Analysis of a Multiple-Frame Highway Bridge in the 1994 Northridge Earthquake.* Gregory L. Fenves and Michael Ellery. December 1998.

- PEER 1998/07** *Empirical Evaluation of Inertial Soil-Structure Interaction Effects.* Jonathan P. Stewart, Raymond B. Seed, and Gregory L. Fenves. November 1998.
- PEER 1998/06** *Effect of Damping Mechanisms on the Response of Seismic Isolated Structures.* Nicos Makris and Shih-Po Chang. November 1998.
- PEER 1998/05** *Rocking Response and Overturning of Equipment under Horizontal Pulse-Type Motions.* Nicos Makris and Yiannis Roussos. October 1998.
- PEER 1998/04** *Pacific Earthquake Engineering Research Invitational Workshop Proceedings, May 14–15, 1998: Defining the Links between Planning, Policy Analysis, Economics and Earthquake Engineering.* Mary Comerio and Peter Gordon. September 1998.
- PEER 1998/03** *Repair/Upgrade Procedures for Welded Beam to Column Connections.* James C. Anderson and Xiaojing Duan. May 1998.
- PEER 1998/02** *Seismic Evaluation of 196 kV Porcelain Transformer Bushings.* Amir S. Gilani, Juan W. Chavez, Gregory L. Fenves, and Andrew S. Whittaker. May 1998.
- PEER 1998/01** *Seismic Performance of Well-Confined Concrete Bridge Columns.* Dawn E. Lehman and Jack P. Moehle. December 2000.

PEER REPORTS: ONE HUNDRED SERIES

The following PEER reports are available by Internet only at http://peer.berkeley.edu/publications/peer_reports_complete.html.

- PEER 2012/103** *Performance-Based Seismic Demand Assessment of Concentrically Braced Steel Frame Buildings*. Chui-Hsin Chen and Stephen A. Mahin. December 2012.
- PEER 2012/102** *Procedure to Restart an Interrupted Hybrid Simulation: Addendum to PEER Report 2010/103*. Vesna Terzic and Božidar Stojadinovic. October 2012.
- PEER 2012/101** *Mechanics of Fiber Reinforced Bearings*. James M. Kelly and Andrea Calabrese. February 2012.
- PEER 2011/107** *Nonlinear Site Response and Seismic Compression at Vertical Array Strongly Shaken by 2007 Niigata-ken Chuetsu-oki Earthquake*. Eric Yee, Jonathan P. Stewart, and Kohji Tokimatsu. December 2011.
- PEER 2011/106** *Self Compacting Hybrid Fiber Reinforced Concrete Composites for Bridge Columns*. Pardeep Kumar, Gabriel Jen, William Trono, Marios Panagiotou, and Claudia Ostertag. September 2011.
- PEER 2011/105** *Stochastic Dynamic Analysis of Bridges Subjected to Spatially Varying Ground Motions*. Katerina Konakli and Armen Der Kiureghian. August 2011.
- PEER 2011/104** *Design and Instrumentation of the 2010 E-Defense Four-Story Reinforced Concrete and Post-Tensioned Concrete Buildings*. Takuya Nagae, Kenichi Tahara, Taizo Matsumori, Hitoshi Shiohara, Toshimi Kabeyasawa, Susumu Kono, Minehiro Nishiyama (Japanese Research Team) and John Wallace, Wassim Ghannoum, Jack Moehle, Richard Sause, Wesley Keller, Zeynep Tuna (U.S. Research Team). June 2011.
- PEER 2011/103** *In-Situ Monitoring of the Force Output of Fluid Dampers: Experimental Investigation*. Dimitrios Konstantinidis, James M. Kelly, and Nicos Makris. April 2011.
- PEER 2011/102** *Ground-Motion Prediction Equations 1964–2010*. John Douglas. April 2011.
- PEER 2011/101** *Report of the Eighth Planning Meeting of NEES/E-Defense Collaborative Research on Earthquake Engineering*. Convened by the Hyogo Earthquake Engineering Research Center (NIED), NEES Consortium, Inc. February 2011.
- PEER 2010/111** *Modeling and Acceptance Criteria for Seismic Design and Analysis of Tall Buildings*. Task 7 Report for the Tall Buildings Initiative - Published jointly by the Applied Technology Council. October 2010.
- PEER 2010/110** *Seismic Performance Assessment and Probabilistic Repair Cost Analysis of Precast Concrete Cladding Systems for Multistory Buildings*. Jeffrey P. Hunt and Božidar Stojadinovic. November 2010.
- PEER 2010/109** *Report of the Seventh Joint Planning Meeting of NEES/E-Defense Collaboration on Earthquake Engineering. Held at the E-Defense, Miki, and Shin-Kobe, Japan, September 18–19, 2009*. August 2010.
- PEER 2010/108** *Probabilistic Tsunami Hazard in California*. Hong Kie Thio, Paul Somerville, and Jascha Polet, preparers. October 2010.
- PEER 2010/107** *Performance and Reliability of Exposed Column Base Plate Connections for Steel Moment-Resisting Frames*. Ady Aviram, Božidar Stojadinovic, and Armen Der Kiureghian. August 2010.
- PEER 2010/106** *Verification of Probabilistic Seismic Hazard Analysis Computer Programs*. Patricia Thomas, Ivan Wong, and Norman Abrahamson. May 2010.
- PEER 2010/105** *Structural Engineering Reconnaissance of the April 6, 2009, Abruzzo, Italy, Earthquake, and Lessons Learned*. M. Selim Günay and Khalid M. Mosalam. April 2010.
- PEER 2010/104** *Simulating the Inelastic Seismic Behavior of Steel Braced Frames, Including the Effects of Low-Cycle Fatigue*. Yuli Huang and Stephen A. Mahin. April 2010.
- PEER 2010/103** *Post-Earthquake Traffic Capacity of Modern Bridges in California*. Vesna Terzic and Božidar Stojadinović. March 2010.
- PEER 2010/102** *Analysis of Cumulative Absolute Velocity (CAV) and JMA Instrumental Seismic Intensity (I_{JMA}) Using the PEER–NGA Strong Motion Database*. Kenneth W. Campbell and Yousef Bozorgnia. February 2010.
- PEER 2010/101** *Rocking Response of Bridges on Shallow Foundations*. Jose A. Ugalde, Bruce L. Kutter, and Boris Jeremic. April 2010.
- PEER 2009/109** *Simulation and Performance-Based Earthquake Engineering Assessment of Self-Centering Post-Tensioned Concrete Bridge Systems*. Won K. Lee and Sarah L. Billington. December 2009.

- PEER 2009/108** *PEER Lifelines Geotechnical Virtual Data Center.* J. Carl Stepp, Daniel J. Ponti, Loren L. Turner, Jennifer N. Swift, Sean Devlin, Yang Zhu, Jean Benoit, and John Bobbitt. September 2009.
- PEER 2009/107** *Experimental and Computational Evaluation of Current and Innovative In-Span Hinge Details in Reinforced Concrete Box-Girder Bridges: Part 2: Post-Test Analysis and Design Recommendations.* Matias A. Hube and Khalid M. Mosalam. December 2009.
- PEER 2009/106** *Shear Strength Models of Exterior Beam-Column Joints without Transverse Reinforcement.* Sangjoon Park and Khalid M. Mosalam. November 2009.
- PEER 2009/105** *Reduced Uncertainty of Ground Motion Prediction Equations through Bayesian Variance Analysis.* Robb Eric S. Moss. November 2009.
- PEER 2009/104** *Advanced Implementation of Hybrid Simulation.* Andreas H. Schellenberg, Stephen A. Mahin, Gregory L. Fenves. November 2009.
- PEER 2009/103** *Performance Evaluation of Innovative Steel Braced Frames.* T. Y. Yang, Jack P. Moehle, and Božidar Stojadinovic. August 2009.
- PEER 2009/102** *Reinvestigation of Liquefaction and Nonliquefaction Case Histories from the 1976 Tangshan Earthquake.* Robb Eric Moss, Robert E. Kayen, Liyuan Tong, Songyu Liu, Guojun Cai, and Jiaer Wu. August 2009.
- PEER 2009/101** *Report of the First Joint Planning Meeting for the Second Phase of NEES/E-Defense Collaborative Research on Earthquake Engineering.* Stephen A. Mahin et al. July 2009.
- PEER 2008/104** *Experimental and Analytical Study of the Seismic Performance of Retaining Structures.* Linda Al Atik and Nicholas Sitar. January 2009.
- PEER 2008/103** *Experimental and Computational Evaluation of Current and Innovative In-Span Hinge Details in Reinforced Concrete Box-Girder Bridges. Part 1: Experimental Findings and Pre-Test Analysis.* Matias A. Hube and Khalid M. Mosalam. January 2009.
- PEER 2008/102** *Modeling of Unreinforced Masonry Infill Walls Considering In-Plane and Out-of-Plane Interaction.* Stephen Kadysiewski and Khalid M. Mosalam. January 2009.
- PEER 2008/101** *Seismic Performance Objectives for Tall Buildings.* William T. Holmes, Charles Kircher, William Petak, and Nabih Youssef. August 2008.
- PEER 2007/101** *Generalized Hybrid Simulation Framework for Structural Systems Subjected to Seismic Loading.* Tarek Elkhoraibi and Khalid M. Mosalam. July 2007.
- PEER 2007/100** *Seismic Evaluation of Reinforced Concrete Buildings Including Effects of Masonry Infill Walls.* Alidad Hashemi and Khalid M. Mosalam. July 2007.

The Pacific Earthquake Engineering Research Center (PEER) is a multi-institutional research and education center with headquarters at the University of California, Berkeley. Investigators from over 20 universities, several consulting companies, and researchers at various state and federal government agencies contribute to research programs focused on performance-based earthquake engineering.

These research programs aim to identify and reduce the risks from major earthquakes to life safety and to the economy by including research in a wide variety of disciplines including structural and geotechnical engineering, geology/seismology, lifelines, transportation, architecture, economics, risk management, and public policy.

PEER is supported by federal, state, local, and regional agencies, together with industry partners.



PEER Core Institutions

University of California, Berkeley (Lead Institution)
California Institute of Technology
Oregon State University
Stanford University
University of California, Davis
University of California, Irvine
University of California, Los Angeles
University of California, San Diego
University of Nevada, Reno
University of Southern California
University of Washington

PEER reports can be ordered at <https://peer.berkeley.edu/peer-reports> or by contacting

Pacific Earthquake Engineering Research Center
University of California, Berkeley
325 Davis Hall, Mail Code 1792
Berkeley, CA 94720-1792
Tel: 510-642-3437
Email: peer_center@berkeley.edu

ISSN 2770-8314
<https://doi.org/10.55461/UUUE2614>